Geoderma 329 (2018) 91–107

Contents lists available at ScienceDirect

Geoderma

journal homepage: www.elsevier.com/locate/geoderma

Small-scale spatial patterns of soil organic carbon and nitrogen stocks in permafrost-affected soils of northern Siberia

Alevtina Evgrafova[a,b,*], Tilman René de la Haye[a], Ina Haase[c], Olga Shibistova[c,d], Georg Guggenberger[c,d], Nikita Tananaev[e], Leopold Sauheitl[c], Sandra Spielvogel[a,f]

[a] Soil Science Group, Geography Department, University of Bern, Bern, Switzerland
[b] Institute for Integrated Natural Sciences, Germany Geography Department, University of Koblenz-Landau, Koblenz, Germany
[c] Institute of Soil Science, Leibniz Universität Hannover, Hanover, Germany
[d] VN Sukachev Institute of Forest, SB-RAS, Akademgorodok, Krasnoyarsk, Russian Federation
[e] Igarka Geocryology Laboratory, Melnikov Permafrost Institute, Yakutsk, Russia
[f] Department of Soil Science and Plant Nutrition, Christian-Albrechts-University of Kiel, Kiel, Germany

ARTICLE INFO

Handling Editor: I. Kögel-Knabner

ABSTRACT

The vulnerability of soil organic matter (SOM) sequestered in permafrost-affected soils to climate change plays one of the key roles in the global carbon (C) cycle. However, it still remains unclear how changing soil and site-specific factors, associated with the changing depth of the permafrost table due to thawing, influence the spatial distribution and variability of soil organic carbon (SOC) and total nitrogen (N) stocks in high-latitude mineral soils.

The relationships between the spatial variation of SOC and N stocks (0–30 cm) and active layer (AL) thickness, thickness of the organic layer (OL), soil acidity, Al and Fe hydroxides as well as plant- and microbial-derived C inputs were studied using ordinary statistics and geostatistics within six landscape patches (16 m^2) in the Siberian forest-tundra ecotone underlain by warm and discontinuous permafrost.

At deeper permafrost table, SOC and N stocks (0–30 cm) were lower and, according to the semivariogram analysis, an overall homogenization of SOC and N distribution at the analyzed scale occurred. Total N and SOC stocks were spatially independent from root-derived organic matter distribution (*i.e.* the concentration of suberin-derived monomers) at shallow AL patches, whereas there was a significant positive spatial correlation within deep AL and non-permafrost soils. Hence, the development of root systems and an increase in rooting depth, leading to "hot spots" of SOM accumulation at intensively rooted soil patches, was observed as a result of deeper AL. Total N and SOC stocks within deeper AL and non-permafrost subsoils were also positively spatially correlated with the concentration of Fe and Al hydroxides, demonstrating the importance of organo-mineral associations for SOM stabilization in soils with lower permafrost table. This study confirmed that deepening of the AL in boreal forest ecosystems may lead to an overall homogenization of SOM distribution and simultaneous development of distinct mechanisms of SOM accumulation and stabilization.

1. Introduction

Although the permafrost-affected soils of the Northern Hemisphere occupy only about 15% of the global soil surface, with up to 1035 ± 150 Pg of soil organic carbon (SOC) in the first 300 cm (Hugelius et al., 2014), they represent about 40% of the global soil C pool (Ping et al., 2015). Climate change-induced progressive deepening of seasonally thawing active layer (AL) in permafrost regions due to rising temperatures during the Arctic summer (IPCC, 2007) may change soil abiotic and biotic conditions and, thus, amplify the magnitude and rate of soil organic matter (SOM) mineralization. For example, warming and increased oxygen availability caused by improved soil drainage directly may accelerate soil microbial activity (Lawrence et al., 2015; Schuur et al., 2015) as well as alter soil microbial community composition, and functional diversity (Deng et al., 2015; Yang et al., 2017; Yuan et al., 2018). In addition, increasing above- and belowground plant productivity associated with warming-driven ecosystem dynamics may induce priming effects and, hence, the mobilization of "old" carbon

* Corresponding author at: Soil Science Group, Geography Department, University of Bern, Bern, Switzerland.
E-mail addresses: alevtina.evgrafova@gmail.com (A. Evgrafova), tilman.delahaye@giub.unibe.ch (T.R. de la Haye), haase@ifbk.uni-hannover.de (I. Haase), olgas@ifbk.uni-hannover.de (O. Shibistova), guggenberger@ifbk.uni-hannover.de (G. Guggenberger), sauheitl@ifbk.uni-hannover.de (L. Sauheitl), s.spielvogel@soils.uni-kiel.de (S. Spielvogel).

https://doi.org/10.1016/j.geoderma.2018.05.014
Received 31 October 2017; Received in revised form 30 March 2018; Accepted 12 May 2018
Available online 29 May 2018
0016-7061/ © 2018 Elsevier B.V. All rights reserved.

(C) as a result of permafrost thaw (Schuur et al., 2009, 2015; Wild et al., 2016). Moreover, the accelerated SOM decomposition may increase the availability of nutrients, which would magnify the direct effects of warming and oxygen availability on microbial activity as well as further stimulate plant productivity (Beermann et al., 2016; Buckeridge et al., 2016; Finger et al., 2016; Salmon et al., 2016). Hence, such a potential shift of permafrost-affected soils from a C sink to a C source may result in a positive climate feedback (Bischoff et al., 2016; Ping et al., 2015; Tarnocai et al., 2009; Webb et al., 2016). At the same time, alteration of belowground processes may lead to the development of a more complex soil structure in former permafrost soil layers and the formation of pedogenic reactive minerals and organo-mineral associations. The latter may, at least partly, counterbalance SOC losses in the long term (Höfle et al., 2013; Kawahigashi et al., 2006; Mueller et al., 2017; Schmidt et al., 2011; Striegl et al., 2005).

Most of the key factors that determine the magnitude, rates of SOM input and mineralization as well as sequestration potential of high-latitude soils have one crucial characteristic in common – high spatial variability at different scales (Gentsch et al., 2015a; Lipson et al., 2015; Loranty et al., 2016; Mueller et al., 2017; Pastick et al., 2014). The majority of previous studies, focusing on the spatial variation of soil properties in permafrost ecosystems, have been conducted in (i) polygonal tundra ecotones (Kutzbach et al., 2004; Wainwright et al., 2015), where the distribution of SOC stocks is dominated by the position within the polygon relief (Gundelwein et al., 2007), (ii) peatlands and areas with thaw-lake basins (Bockheim and Hinkel, 2007; Van Bellen et al., 2011), (iii) mountainous boreal forests, where topography dominates SOC and N spatial pattern (Baumann et al., 2009; Hoffmann et al., 2014), or (iv) with a focus on the spatial variability of SOC stocks in organic layer (OL) of boreal forest soils (Häkkinen et al., 2011; Kristensen et al., 2015; Muukkonen et al., 2009), while the mineral soil horizons are being underrepresented. A better knowledge on the parameters determining the spatial patterns of SOM in permafrost soils at resolutions smaller than the landscape-scale would increase the understanding of the processes defining the spatial variability and enable better prediction of possible environmental impacts associated with permafrost thaw (Hobbie et al., 2000; Neff and Hooper, 2002; Ping et al., 2015; Schuur et al., 2015). The estimation of the small-scale spatial variability of SOC and nitrogen (N) stocks and their composition in high-latitude soils would also improve the accuracy of SOC and N inventories for the circumpolar regions (Lal, 2009; Vanguelova et al., 2016; Wang and Hsieh, 2002) and the upscaling procedure from the pedon to the stand scale (Banfield et al., 2002; Finke et al., 2002; Hatfield, 2001). The global environmental models could also be improved by including the small-scale vertical and horizontal heterogeneity of soil properties in sampling designs, geospatial upscaling and soil mapping approaches (Gentsch et al., 2015b; Hugelius, 2012; Hugelius et al., 2011; Köchy et al., 2015; Mishra and Riley, 2012, 2015; Ping et al., 2015; Zubrzycki et al., 2013). Despite studies that focused on the catchment scale variability (Fuchs et al., 2009; Harms et al., 2016; Rodionov et al., 2007), little is known about the spatial variability of SOC and N stocks in boreal forests at smaller spatial scales. Therefore, high-resolution mapping of the soil parameters such as the thicknesses of AL and OL, pH, pedogenic reactive minerals, and quantity and quality of above- and belowground organic matter (OM) inputs to the mineral permafrost-affected soils could assist in identifying the factors controlling SOC and N stocks in Cryosols as well as detecting “hot spots” and understanding the dynamics of SOC stocks and availability of nutrients pertaining to permafrost thaw. After permafrost thaw, accelerated belowground plant productivity may contribute to the formation of spatial distinct root-derived SOM “hot spots” that might be identified by the use of molecular markers. For instance, to differentiate between above- and belowground plant C inputs to soil, cutin- and suberin-derived monomers could be used as accurate and effective tracers (Nierop, 2001; Spielvogel et al., 2014) as the ratio of aboveground-to-belowground OM inputs will likely change with the depth of the AL. Likewise, the ratios between specific sugar monomers could be used as a proxy for estimating the relative contribution of different OM sources (plant- *vs*. microbial-derived OM or higher *vs*. lower plants) to SOM formation as well as the stage of SOM turnover. It has been shown that soil sugars of plant origin are in greater proportion represented by pentoses (*e.g.* arabinose and xylose), while microbial- and moss-derived carbohydrates comprise in greater degree hexoses (*e.g.* galactose and mannose) and deoxy sugars (*e.g.* fucose and rhamnose) (Comont et al., 2006; Delarue et al., 2011; Murayama, 1984; Oades et al., 1984; Prietzel et al., 2013).

In order to understand how permafrost regime influences the short distance spatial structure of SOC and N stocks (0–30 cm) of mineral permafrost soils, six grids of 16 m^2 with varying permafrost regimes and under different vegetation associations were studied in northern Siberia in 2014. The objectives of this research were to characterize the small-scale spatial heterogeneity of SOC and N stocks and to identify its controlling factors by studying the spatial relationships between SOC and N stocks and soil variables such as AL thickness, dithionite-extractable Fe and Al hydroxide content, pH, and above- and belowground originated OM. The latter was measured as the content and composition of total neutral sugars, as well as cutin- and suberin-derived compounds. The hypothesis was that AL thickness is the main factor defining the spatial patterns of SOC and N stocks in permafrost affected mineral soils, while other parameters (*e.g.* content of reactive Fe and Al hydroxides, root-derived C inputs) will have an increasing influence on the spatial distribution of SOC and N stocks with declining permafrost impact.

2. Materials and methods

2.1. Study area

The study was conducted in northern Siberia at the Little Graviyka creek catchment (UTM 45W: 67°28.933′N, 86°25.682′E and 20–38 m a.s.l.), Krasnoyarsk Krai, Russian Federation in August 2014 (Fig. 1). Mean annual temperature in the region was −7.6 °C, and mean annual precipitation was 513 mm for 1973–2013 (Streletskiy et al., 2015). According to Flessa et al. (2008), Guggenberger et al. (2006, 2008) and Rodionov et al. (2007), the study catchment is located within a zone of warm (−1 °C–0 °C) discontinuous permafrost in the forest-tundra subzone of the boreal zone. The study catchment is characterized by a high temporal and spatial variability of permafrost features such as AL thickness, drainage conditions, and vegetation associations (Rodionov et al., 2007). The soil parent materials are homogeneous and characterized as silty Late Pleistocene fluvio-glacial (Karginskaya interstage) and limnic sediments (Zyryansk epoch). The area is characterized by northern open woodlands dominated by Siberian spruce (*Picea obovata* Ledeb.), silver birch (*Betula pendula* Roth.), and Siberian larch (*Larix sibirica* Ledeb.). The north-facing slopes are covered by sparser mixed forest species, while the south-facing slopes are characterized by denser forest stands and deeper AL thickness.

2.2. Study grids and sampling design

For the reason of high variability of soil properties, six plots of four by four meters (16 m^2), further named as study grids, were identified in order to represent the majority of possible combinations of factors defining the spatial heterogeneity of SOC and N stocks such as slope orientation, AL thickness, and vegetation associations (Table 1). No signs of active cryoturbation were observed within the upper 30 cm of mineral soils at the six study grids. The analysis of variance allowed to divide the study grids into four groups based on AL thickness: One grid underlain by shallow AL (PF1, AL thickness is about 40 cm from the surface down to the permafrost table), two grids with intermediate AL (PF2 and PF3, 50 cm on average), one grid underlain by a deeper AL (PF4, 65 cm), and two grids with no presence of permafrost within the

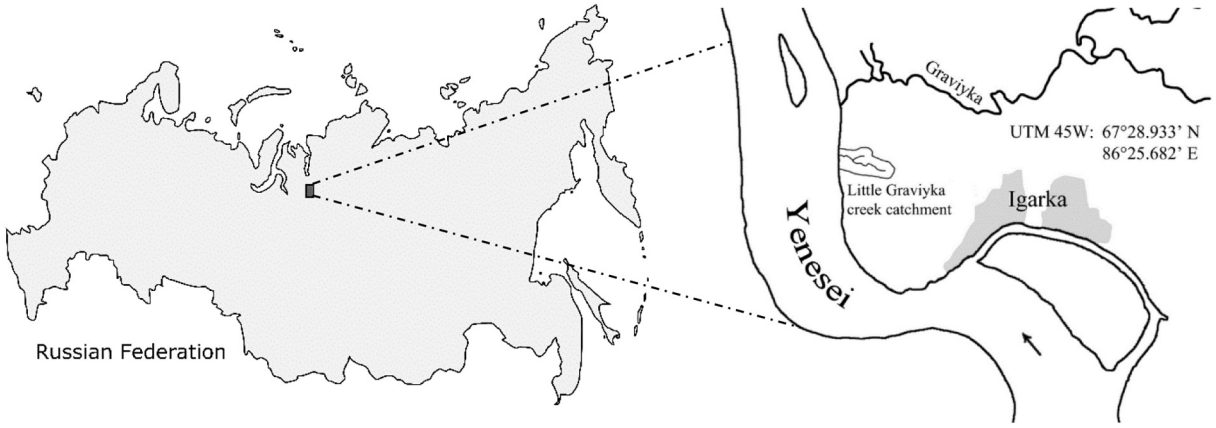

Fig. 1. The study area, the Little Graviyka creek catchment (UTM 45W: 67°28.933′N, 86°25.682′E), located within a zone of warm and discontinuous permafrost in the forest-tundra subzone of the boreal zone, and approximately 6 km to the northwest of Igarka city, Krasnoyarsk Krai, Russian Federation. (adapted from the topographic map of Turukhansk District, Q45).

upper 100 cm layer (NP1 and NP2) (Table 2).

The understory and forest floor vegetation within the six study grids were represented by shrubs (*Ledum palustre* L., *Vaccinium* spp.), peat (*Sphagnum* spp.) and hair (*Polytrichum* spp.) mosses, horsetail (*Equisetum* spp.), and sedges (*Carex* spp.) (Table 1). The permafrost-affected grids were, in addition, characterized by presence of perennial herbs such as cloudberry (*Rubus chamaemorus* L.), while reindeer lichen (*Cladonia rangiferina* L.) was present within grids PF1, PF4 and NP2. The dwarf birch (*Betula nana* L.) and downy willow (*Salix lapponum* L.) shrubs were found only within grid PF2. The soils were classified according to the World Reference Base for Soil Resources (Table 1) (IUSS Working Group WRB, 2014).

Soil and plant samples from the most abundant plant species of each site (*Picea obovate* Ledeb., *Larix sibirica* Ledeb., *Betula pendula* Roth., *Betual nana* L., *Ledum palustre* L., *Vaccinium* spp., *Sphagnum* spp., *Polytrichum* spp., *Equisetum* spp., *Carex* spp.) were taken in August 2014 when the annual thaw depth was at its maximum. Soil samples were obtained from the organic horizon as well as two mineral soil samples, precisely, from the topsoil (referring to Ah horizon) and from the following subsoil horizon, *i.e.* from the lower border of the Ah horizon to 30 cm depth of the mineral soil surface. The square study grid of 16 m^2 was divided into sixteen sub-grids of 1 m^2 (Fig. 2). In order to obtain a high spatial resolution, soil samples were taken using a systematic sampling approach in the corners (corner samples, n = 25) and centers (centered samples, n = 16) of each sub-grid. In addition, 20 nested samples were randomly collected in order to include characteristics such as micro-relief or tree locations within each study grid. Spatially referenced mineral soil samples (n = 731) were taken separately at 61 sampling points within each study grid using a steel soil corer (5 cm Ø, 34 cm long) with a sample spacing ranging between 0.2 and 5.7 m. Hence, 122 mineral soil samples were collected for each study grid, with an exception of 121 soil samples for grid PF4. The OL samples (n = 12) were collected for each study grid as two mixed samples from the corner and centered sample points. During the soil core sampling process, the thicknesses of OL and topsoil for each sampling point were determined.

2.3. Analysis of basic soil physical and chemical properties

The OL samples and mineral soil samples were air-dried directly after sampling. All visible roots were removed, and soil samples were sieved (< 2 mm) prior to chemical analysis. The coarse fragment (*CF*) content (> 2 mm size) was determined and used for further calculations of the OC and N stocks. The air-dried mineral soil and OL samples were ground with an agate mortar and a ball mill, respectively, prior to elemental analysis. Soil pH values of corner and centered soil samples were measured at room temperature using 0.01 M $CaCl_2$ suspension at the ratios of 1:10 and 1:2 (*v:v*) for mineral top- and subsoils, respectively. The SOC and total N content (in % soil dry weight) were determined by dry combustion using an elemental analyzer (Vario EL

Table 1
The main characteristics of the six study grids: four permafrost sites (PF1–PF4) and two sites with no permafrost within the upper 100 cm layer (NP1 and NP2).

Parameter		PF1	PF2	PF3	PF4	NP1	NP2
Longitude[a]		N 7485120	N 7485087	N 7485182	N 7485226	N 7485272	N 7485339
Latitude[a]		E 475674	E 475604	E 475643	E 475568	E 475479	E 475595
Slope orientation		NW	NW	NW	NW	NW	SE
AL, cm		39.8 ± 0.03 a	49.5 ± 0.04 b	50.5 ± 0.03 b	64.6 ± 0.03 c	NP d	NP d
Dominant plant species	Tree species	*Picea obovata*, *Larix sibirica*, *Betula pendula*	*Picea obovata*, *Betula pendula*	*Picea obovata*, *Betula pendula*	*Picea obovata*, *Betula pendula*	*Picea obovata*, *Larix sibirica* (higher abundance)	*Picea obovate*, *Larix sibirica*, *Betula pendula* (higher abundance)
	Understory and ground cover	*Ledum palustre*, *Vaccinium* spp., *Sphagnum* spp., *Polytrichum* spp., *Carex* spp., *Equisetum* spp.					
		Cladonia rangiferina, *Rubus chamaemorus*	*Betula nana*, *Salix lapponum*, *Rubus chamaemorus*	*Rubus chamaemorus*	*Cladonia rangiferina*, *Rubus chamaemorus*	–	*Cladonia rangiferina*
Number of soil samples taken		122	122	122	121	122	122
Soil type (IUSS Working Group WRB, 2014)		Umbric Histic Cryosols (Nechic, Profundihumic)	Umbric Histic Cryosols (Nechic, Profundihumic)	Umbric Histic Cryosols (Nechic, Profundihumic)	Umbric Histic Cryosols (Nechic, Profundihumic)	Leptic Histic Stagnic Cambisols (Colluvic, Profundihumic)	Leptic Histic Stagnic Cambisols (Protospodic, Profundihumic)

[a] Grid locations were measured using the Universal Transverse Mercator coordinate system (UTM), zone 45W with the central meridian 87° E on The Ashtech® ProMark2™; AL – active layer thickness; NP – no permafrost within the upper 100 cm layer.

Table 2
The mean values with standard errors in brackets for diagnostic, chemical and physical soil properties for the six study grids, where PF1 to PF4 are grids with permafrost-affected soils and NP1 and NP2 are grids with no presence of permafrost within the upper 100 cm layer. Different letters represent statistical differences ($P \leq 0.05$) for mean values among the six study grids.

Parameter	Soil layer	PF1		PF2		PF3		PF4		NP1		NP2		n
Thickness,	OL	17.7 (0.5)	cd	17.9 (0.4)	d	16.4 (0.3)	c	18.4 (0.4)	d	13.2 (0.3)	b	10.4 (0.3)	a	61
cm	Topsoil	3.7 (0.2)	a	5.5 (0.3)	b	4.7 (0.3)	b	3.6 (0.2)	a	3.6 (0.2)	a	4.8 (0.2)	b	61
C:N	OL	36.6 (0.3)	c	37.4 (0.2)	cd	33.8 (0.2)	b	38.6 (0.1)	e	31.7 (0.2)	a	37.6 (0.2)	d	36
	Topsoil	20.3 (0.4)	b	20.2 (0.2)	b	19.2 (0.3)	a	20.0 (0.3)	ab	22.3 (0.4)	c	27.0 (0.5)	d	61
	Subsoil	14.6 (0.1)	a	18.3 (0.2)	c	15.5 (0.2)	b	15.7 (0.2)	b	18.3 (0.3)	c	19.7 (0.3)	d	61
pH_{CaCl2}	Topsoil	4.45 (0.10)	e	3.81 (0.05)	c	4.31 (0.07)	e	4.06 (0.07)	d	3.67 (0.05)	b	3.48 (0.03)	a	41
	Subsoil	5.53 (0.06)	d	4.64 (0.06)	b	5.36 (0.03)	d	5.00 (0.04)	c	4.59 (0.04)	b	4.34 (0.03)	a	41
BD,	0–10 cm	1.10 (0.06)							b	0.94 (0.00)			a	6|3
$g\,cm^{-3}$	10–30 cm	1.17 (0.07)							a	1.13 (0.03)			a	2|4
SOC,	OL	6.51 (0.19)	c	7.11 (0.23)	cd	6.47 (0.19)	cd	7.77 (0.25)	d	5.07 (0.17)	b	3.62 (0.15)	a	61
$kg\,C\,m^{-2}$	Topsoil	4.96 (0.48)	bc	6.53 (0.60)	cd	6.93 (0.60)	d	3.07 (0.31)	a	3.45 (0.21)	ab	4.49 (0.22)	cd	61
	Subsoil	9.01 (0.37)	cd	10.42 (0.48)	d	7.76 (0.53)	ab	6.30 (0.24)	a	7.89 (0.34)	bc	5.49 (0.13)	a	61
	0–30 cm	13.97 (0.66)	c	16.95 (0.70)	d	14.69 (0.78)	c	9.37 (0.34)	a	11.34 (0.42)	b	9.98 (0.26)	ab	122
	Total	20.48 (0.66)	c	24.06 (0.73)	bc	21.16 (0.79)	bc	17.15 (0.43)	b	16.41 (0.47)	a	13.59 (0.28)	a	122
N,	OL	0.18 (0.01)	c	0.19 (0.01)	cd	0.19 (0.01)	c	0.20 (0.01)	d	0.16 (0.00)	b	0.10 (0.00)	a	61
$kg\,N\,m^{-2}$	Topsoil	0.25 (0.02)	bc	0.32 (0.03)	cd	0.35 (0.03)	d	0.16 (0.02)	a	0.16 (0.01)	a	0.17 (0.01)	ab	61
	Subsoil	0.61 (0.02)	c	0.56 (0.02)	c	0.48 (0.03)	b	0.40 (0.01)	b	0.43 (0.02)	b	0.28 (0.01)	a	61
	0–30 cm	0.86 (0.03)	c	0.89 (0.03)	c	0.83 (0.04)	c	0.55 (0.02)	b	0.58 (0.02)	b	0.45 (0.01)	a	122
	Total	1.03 (0.03)	d	1.07 (0.03)	cd	1.02 (0.03)	d	0.76 (0.02)	c	0.74 (0.21)	b	0.54 (0.11)	a	122
$Al_d + 0.5\,Fe_d$,	Topsoil	31.28 (2.20)	d	10.04 (0.33)	c	9.64 (0.38)	c	5.90 (0.21)	a	7.00 (0.25)	b	6.89 (0.25)	b	61
$mg\,g^{-1}$	Subsoil	8.06 (0.34)	c	5.45 (0.13)	b	6.63 (0.11)	d	6.79 (0.23)	d	4.58 (0.16)	a	7.31 (0.25)	cd	61

n – the amount of samples per study grid; for PF4: n is equal to n-1; OL – organic layer; BD – bulk density; SOC – soil organic carbon stock; N –total nitrogen stock; $Al_d + 0.5\,Fe_d$ – dithionite-extractable pedogenic iron and aluminum hydroxides.

cube, CHN mode, Elementar Analysensysteme GmbH, Hanau, Germany). The mineral soil samples were tested for presence of inorganic C by means of the Scheibler apparatus (DIN ISO 10693). If necessary, the latter was removed prior to the elemental analysis using the volatilization method (hydrochloric acid, 6 h) based on Hedges and Stern (1984) and Harris et al. (2001). Dithionite-extractable Fe and Al hydroxides (Fe_d and Al_d) were determined using the dithionite-citrate-bicarbonate method (Holmgren, 1967). The measurements were done on an inductively coupled plasma mass spectrometer (ICP-MS 7700X; Agilent Technologies, Waldbronn, Germany). The value 0.5 was used to sum Al_d and Fe_d on a molar basis ($Al_d + 0.5\,Fe_d$). SOC and total N stocks ($kg\,m^{-2}$) at each sampling point were calculated for the two mineral soil layers (*i.e.* top- and subsoils from 0 to 30 cm) based on Eq. (1),

$$\text{SOC/N stocks (kg OC/N m}^{-2}) = \text{SOC/N} \times \text{BD} \times \text{H} \times (1 - \text{CF}) \times 10^{-2} \quad (1)$$

with SOC/N content ($g\,kg^{-1}$), BD – bulk density ($g\,cm^{-3}$), H – thickness of the soil layer (cm), and *CF* – coarse fragment content (% weight).

2.4. Determination of root-derived suberin and leaf-derived cutin compounds

Plant (n = 19) and mineral soil samples (n = 365) of three selected study grids PF1, PF4 and NP1, representing soil groups with various permafrost impact, were additionally analyzed for cutin- and suberin-

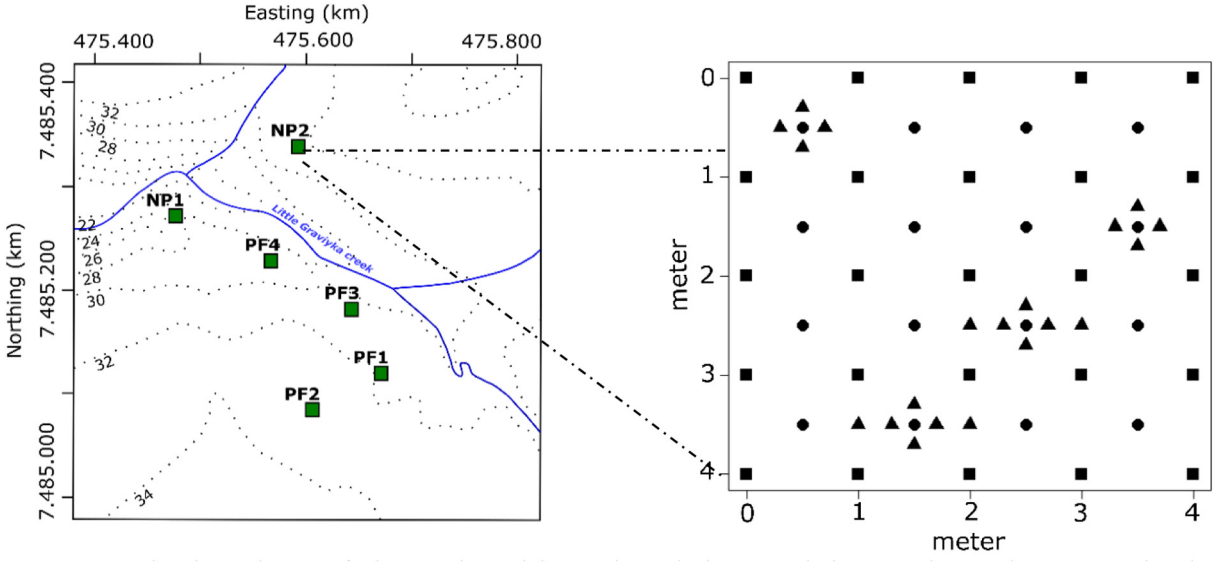

Fig. 2. The locations of six study grids at the Little Graviyka creek catchment and schematic sampling design (*i.e.* NP2 site) of a grid four by four meters. The location of corner (squares, n = 25) and centered (circles, n = 16) sampling points are identical at each grid, while location of nested sampling points (triangles, n = 20) varied among grids and depended on grid special characteristics (*i.e.* micro-relief, tree locations). PF1 to PF4 are grids with permafrost-affected soils and NP1 and NP2 are grids with no presence of permafrost within 100 cm layer.

derived lipid composition and content as well as non-cellulosic neutral sugars content (Section 2.5). The study grids for cutin, suberin and neutral sugar analyses were selected in order to study the differences in spatial variation and compound pools induced by different AL depth and vegetation association (Fig. 1). The sequential chemical extraction of cutin- and suberin-derived lipids was based on a modified method described by Otto and Simpson (2007) and Spielvogel et al. (2014). Depending on SOC content, 0.46 to 3.00 g of mineral soil or 0.04 g of plant material was subjected to alkaline hydrolysis using 15 mL of 1 M potassium hydroxide in methanol at 100 °C for 3 h in teflon-lined bombs. After cooling, the samples were centrifuged for 15 min at 841 RCF and the supernatant, containing suberin and cutin monomers, was collected with a Pasteur pipette. The residue was extracted twice by sonication for 15 min with 10 mL dichloromethane:methanol (1:1; v/v) and for a third time with pure dichloromethane, subsequently centrifuged for 20 min at 841 RCF and the supernatant was collected after each extraction step. All supernatants of one sample were combined. To compensate for any losses during analysis of cutin and suberin monomers, 25 µL of octadecanoic acid ($3 \times {}^{2}H$, concentration 1.2 mg mL^{-1}), 25 µL of hexadecanedioic acid ($28 \times {}^{2}H$, concentration 1.2 mg mL^{-1}) and 20 µL of 17-hydroxyheptadecanoic acid (concentration 1.2 mg mL^{-1}) were added as internal standards (IS1-3).

To achieve separation, distilled water (25 mL) was added to the combined supernatants. The upper aqueous phase was acidified to pH 1 with 6 M hydrochloric acid and the organic phase was collected and evaporated to dryness. Afterwards, the samples were re-dissolved with dichloromethane and transferred into 3 mL glass vials, air-dried and stored at −20 °C until derivatization. For derivatization the samples were re-dissolved in dichloromethane and methylized using 500 µL of boron trifluoride at 60 °C for 20 min. After cooling to room temperature, 500 µL of sodium chloride and 1 mL of hexane were added for liquid-liquid extraction and the organic phase was obtained after intensive shaking for 30 s and complete phase separation. This step was repeated two times with 1 mL of pure hexane. All supernatants have been combined and evaporated under a N_2 stream. The combined extracts were re-dissolved in 200 µL pyridine and 200 µL of acetic anhydride were added to convert the monomers into their acetyl esters over night at room temperature. Finally, the methylated and acetylated suberin and cutin monomers were obtained by liquid-liquid extraction with 0.8 mL of 4 N hydrochloric acid and 1 mL of hexane. The organic phase was collected and remaining water and acetic acid were removed by solid-state extraction using sodium sulfate filled columns. The liquid-liquid extraction was repeated two times with 1 mL of hexane. The three extracts of each sample were combined and evaporated under a N_2 stream. 15 µL of tridecanoic acid (concentration 1.0 mg mL^{-1}) as internal standard four and 185 µL of toluene were added and the samples were transferred into gas chromatography vials for measurement. The derivatized cutin and suberin monomers were measured using an Agilent GC System 7890A coupled to an Agilent GC/MS 5975C XLEI MSD (Agilent Technologies, Waldbronn, Germany). A DB-5MS column (30 m length, 250 µm inner diameter and 0.25 µm film thickness) was used for the separation of the monomers using Helium 4.6 (ISO 14175:I2) as carrier gas at a flow rate of 1.2 mL min^{-1} and 1 µL of each sample was injected at an injector temperature of 280 °C. The GC operation conditions during the measurement were as follows: temperature was held constant at 80 °C for 1 min after injection, raised by 10 °C min^{-1} to 150 °C, then raised by 1 °C min^{-1} to 275 °C, then raised by 10 °C min^{-1} to 300 °C and held isothermal for 10 min. The individual cutin- and suberin-derived monomers were identified by comparing their mass spectra with the external standards and the National Institute of Standards and Technology (NIST) Mass Spectral library using the MassHunter Workstation Software (version B.0.6). Quantification of the monomers was done by means of external standard calibration, combined with the IS4 to account for variations during measurement and IS1-3 to account for sample losses during sample preparation.

2.5. Determination of non-cellulosic neutral polysaccharide monomers

The non-cellulosic neutral polysaccharide composition of the plant samples and mineral soil samples from the three study grids PF1, PF4 and NP1 was determined by gas chromatography after acid hydrolysis and subsequent alditol acetate derivatization according to Eder et al. (2010). The content of the eight individual non-cellulosic neutral sugars such as arabinose (A), fucose (F), galactose (G), glucose, mannose (M), rhamnose (R), ribose, and xylose (X) was calculated based on external standard calibration series and corrected by the internal standard myo-inositol (Sigma-Aldrich GmbH, Germany). The sum of the eight compounds was further named as the total neutral sugar (TNS) content. Additionally, the ratios of GM/AX and RF/AX were calculated in order to determine the relative contribution of plant and microbial SOM sources (mosses *vs*. other plant species and their parts such as roots, twigs, needles/leaves; Prietzel et al., 2013).

2.6. Statistical and geostatistical analyses

Conventional statistics and geostatistical analyses were done for two mineral soil layers (*i.e.* top- and subsoil) for all of the six study grids using *R*, version 3.1.3 (R Core team, 2015). A critical significance level of $P = 0.05$ was used if not stated otherwise. Prior to the statistical analyses, all data sets were tested for normality using the Shapiro-Wilk test and by interpreting the QQ and density plots as well as the skewness and kurtosis of each investigated soil variable. The Levene's test was used in order to test the homogeneity of variance. If normality was not observed, as in most cases, the non-parametric equivalents of the analysis were applied. In order to study the influence of top-down permafrost thawing (*i.e.* AL thickness deepening) on measured variables within top- and subsoils, either a parametric one-way repeated measures analysis of variance (ANOVA) or nonparametric Kruskal-Wallis test was applied. The effects of the six study grids were distinguished by a Tukey's HSD test and Conover-Iman test including Holm's *P*-value adjustment method, as *post hoc* tests, respectively. The Spearman's *rho* was used for correlation analysis for pairwise complete observations ("psych" package). The *P*-values were adjusted using the Holm-Bonferroni method in order to test the multiple correlations between variables per dataset for significance.

The semivariogram analysis was used in order to estimate the spatial patterns of SOC stocks, N stocks, and Fe_d and Al_d contents for the six study grids, while the spatial patterns of cutin, suberin, eight neutral sugars and TNS stocks as well as GM/AX and RF/AX ratios were studied only for the three study grids PF1, PF4 and NP1. If a dataset was not normally distributed, the Cressie's semivariance was used instead of the standard semivariance. The semivariograms, which characterize the spatial correlation of studied soil parameters, were modeled using the spherical function for SOC and N stocks and Matern, circular, linear, pentaspherical and wave functions for all other variables. The goodness of a model fit was estimated by both the root-mean-square error, which was computed using the same data as for the empirical and theoretical variograms, and visual assessment. The spatial structure and degree of spatial dependence of soil properties were assessed using the correlation length (*range*) and the nugget-to-sill (N/S) ratio. The N/S ratio indicates the spatial variance at a distance smaller than the sample spacing and/or due to any measurement errors (*nugget*) as a percentage of the total variance (*sill*) (Diggle, 2008).

The ordinary kriging, as an appropriate interpolation method for most cases (Krasilnikov et al., 2008), was used to illustrate the spatial patterns of studied soil properties.

Based on the IPCC recommendations (IPCC, 2000), the minimum number of samples needed for a required precision or so called the minimum detectable difference of SOC and N stocks could be determined using the following formulas (Baritz et al., 2008; Schöning et al., 2006):

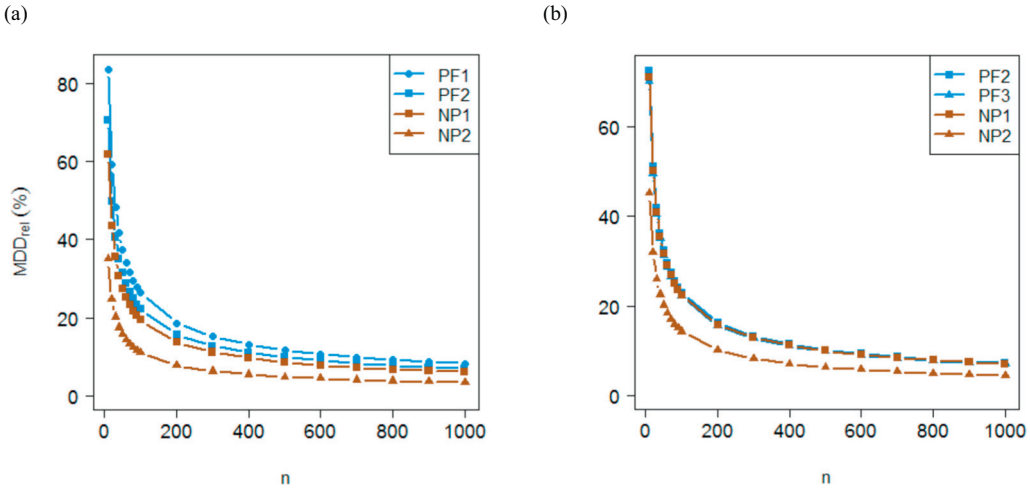

Fig. 3. The relative minimum detectable difference (MDD_{rel}) for (a) SOC stocks and (b) total N stocks in the topsoils in relation to the sample size.

$$MDD\ (unpaired\ samples) \geq \sqrt{\frac{2s_p^2}{n}(t_{\alpha(2),\nu} + t_{\beta(1),\nu})^2} \quad (2)$$

$$MDD\ (rel.) = \frac{MDD}{\bar{x}} \bullet 100\% \quad (3)$$

where MDD is the minimum detectable difference, $s_p{}^2$ is the pooled variance of the two sample sets, n is the sample size and t is the t-statistic at a given significance level (α), β is the probability of type II error, ν is the degree of freedom, and $\bar{x}$ is the mean SOC or N stock (Schöning et al., 2006; Zar, 1984). A statistical power (1 − β) of 0.90 and a significance level (α) of 0.05 were used. In order to estimate the topsoil MDD, it was assumed that SOC and N stocks would be sampled at least at nine sampling points of each study grid. During the second step, it was assumed that the same sampling would be repeated at the distance larger than the range, derived from the previously calculated semivariogram of the respective variable and grid, hence, an unpaired sampling (Fig. 3).

3. Results

3.1. Spatial distribution of soil organic carbon and total nitrogen stocks

Soil OC stocks in the OL were estimated as 4.43 ± 0.22 kg C m^{-2} (± 95% confidence intervals) for non-permafrost (NP1, NP2) and 6.97 ± 0.22 kg C m^{-2} for permafrost-affected soils (PF1-PF4) (Table 2). The permafrost-affected sites were characterized by considerably thicker OL (17.6 ± 0.6 cm, n = 487) in comparison to non-permafrost sites (11.8 ± 0.6 cm, n = 244). The mineral horizons of permafrost-affected soils down to a depth of 30 cm stored between 9.37 (PF4) and 16.95 kg C m^{-2} (PF2), while the SOC stocks (0–30 cm) of non-permafrost soils were accounted for 11.34 and 9.98 kg C m^{-2} at NP1 and NP2 (Table 2). The thickness of the AL in the mineral soil varied between 15.8 and 31.8 cm within the shallow AL grid (PF1), between 24.6 and 41.6 cm for the intermediate grids (PF2-PF3), and between 25.8 and 63.8 cm at site PF4 underlain by deeper permafrost. Based on the ANOVA analysis, SOC stocks (0–30 cm) were divided into two groups; the three sites with high permafrost table (PF1-PF3, AL thickness ≈ 47 cm) and the three other sites with a deep AL (PF4, > 65 cm) and no permafrost within the upper 100 cm layer (NP1 and NP2). The latter group contained significantly ($P \leq 0.01$) lower SOC stock (on average 10.23 ± 0.38 kg C m^{-2}) as compared to the study grids with high and intermediate permafrost table (15.20 ± 0.81 kg C m^{-2}). Despite the small thickness of the topsoil (4.3 ± 0.2 cm, n = 366), among the six study grids, between 30% (NP1) and 47% (PF3) of SOC stocks in the upper 30 cm of mineral soils were stored in the topsoil.

The total N stocks in the OL decreased from 0.19 ± 0.01 kg N m^{-2} in permafrost-affected soils to 0.13 ± 0.01 kg N m^{-2} within non-permafrost study grids. The total N stocks (0–30 cm) in the mineral horizons ranged between 0.45 (NP2) and 0.89 kg N m^{-2} (PF2) (Table 2), and were significantly ($P \leq 0.01$) lower (*i.e.* ≈38%) within non-permafrost (NP1 and NP2) grids and the grid of PF4 with a thicker AL (0.53 ± 0.02 kg N m^{-2}) as compared to the grids with shallow and intermediate AL (PF1-PF3) (0.86 ± 0.04 kg N m^{-2}). In addition, top- and subsoils of permafrost-affected study grids were characterized by lower mean C:N ratios (topsoil: 19.9, n = 244; subsoil: 16.0, n = 243) than non-permafrost soils (topsoil: 24.7, n = 122; subsoil: 19.0, n = 122) (Table 2). The C:N ratios of the mineral soils for all study grids decreased with depth.

The nugget-to-sill (N/S) ratios indicated a strong to moderate spatial dependence structure of SOC and total N stocks among the six study grids, and the semivariogram analysis indicated a decrease in the total variability of SOM stocks with deepening of the AL (Figs. 4, 5). Hence, the non-permafrost study grids and PF4 had a more homogeneous distribution of SOM compared to grids PF1–PF3. The decrease in small-scale spatial heterogeneity of SOC stocks with deeper AL thickness was confirmed by significantly lower mean N/S ratios of topsoil OC stocks within grids PF4, NP1 and NP2 (22%) compared to N/S ratios for shallow and intermediate AL grids, estimated at 36% (Table 3). Moreover, N stocks within grids with lower permafrost impact were also characterized by significantly lower mean N/S ratios of both topsoil (19%) and subsoil (31%) compared to N/S for shallow and intermediate AL grids, estimated at 29% and 52% (Table 3). The N/S ratios were comparable for subsoil OC stocks of the two soil groups with different permafrost impacts. The range of spatial autocorrelation of SOC and total N stocks was comparable for the two soil groups in topsoils and subsoils, however, higher for subsoils compared to topsoils (Table 3).

3.2. Spatial relationship between soil organic carbon stocks, total nitrogen stocks and soil specific factors

Correlation analysis was used to identify the relationships between AL thickness, OL thickness, soil acidity, Al_d + 0.5 Fe_d contents, and SOC or total N stocks in mineral topsoils and subsoils within the study grids (Table 4). Soil OC and total N stocks in both soil layers did not have any significant correlation ($P \leq 0.05$) neither with the thicknesses of AL nor

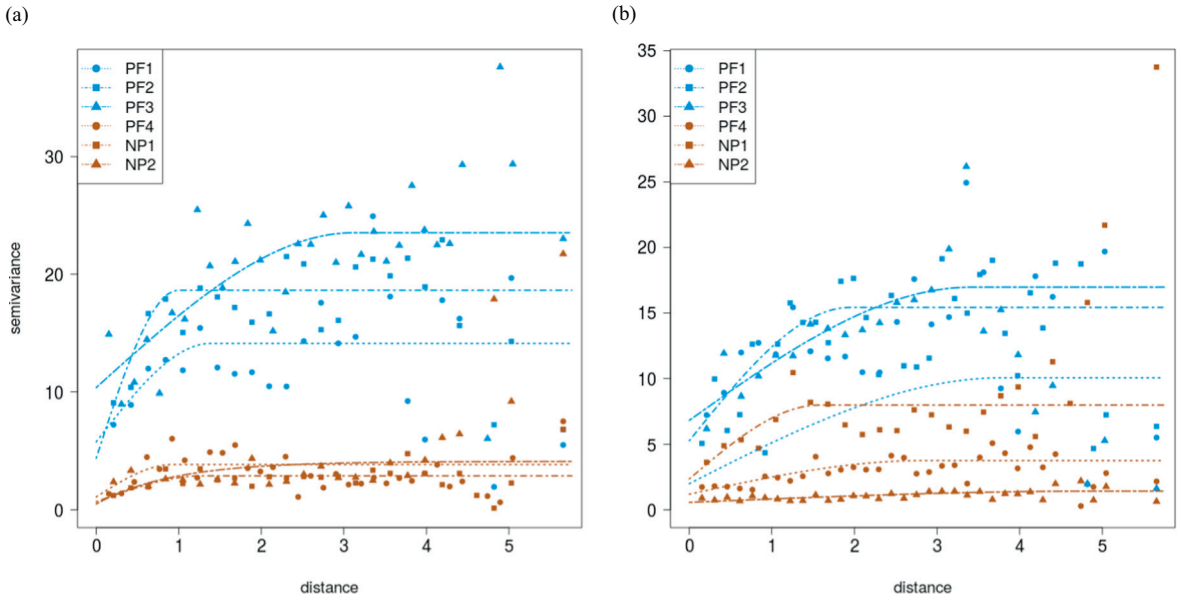

Fig. 4. The semivariograms of (a) topsoil SOC stocks (kg C m^{-2}), (b) subsoil SOC stocks (kg C m^{-2}), obtained for the six study grids (4 × 4 m).

OL within the six study grids (Table 4). The mean pH_{CaCl2} values for both, top- and subsoils, were higher at the permafrost-affected sites (topsoil: 4.16, n = 164; subsoil: 5.13, n = 163) as compared to non-permafrost sites (topsoil: 3.58; subsoil: 4.47, n = 82), with the exception of the subsoil within grid PF2 (Table 2). Additionally, the mean pH_{CaCl2} values of subsoils (down to a depth of 30 cm) for both studied groups, increased by approximately one unit in comparison to those of topsoils. Soil OC and N stocks were moderately correlated ($P \leq 0.05$) with pH only in the topsoil of grid PF2. No significant spatial correlation was found between pH-values and SOC stocks nor with N stocks for the top- and subsoils of the other study grids (Table 4).

The content of Al_d + 0.5 Fe_d ranged between 5.90 mg g^{-1} (PF4) and 31.28 mg g^{-1} (PF1) in the topsoils, and between 4.58 mg g^{-1} (NP1) and 7.31 mg g^{-1} (NP2) in the subsoils within the six grids (Table 2). The contents of Al_d + 0.5 Fe_d were significantly ($P \leq 0.05$) higher in the topsoils within grids PF1–PF3 (16.98 ± 1.12 mg g^{-1}) as compared to the grid with deeper AL or no permafrost impact

Table 3
The semivariogram parameters for the spherical and exponential[a] models fitted in the semivariograms of SOC and total N stocks.

Grid	Soil layer	Semivariogram parameter	SOC	TN
PF1-PF3 (n = 3)	Topsoil	Range (m)	1.83	1.46
		Sill	18.77	0.04
		N/S (%)	36	29
	Subsoil	Range (m)	3.05	2.44
		Sill	14.15	0.04
		N/S (%)	31	52
PF4, NP1, NP2 (n = 3)	Topsoil	Range (m)	1.66	1.49
		Sill	3.62	0.01
		N/S (%)	22	19
	Subsoil	Range (m)	3.11	2.99
		Sill	4.39	0.02
		N/S (%)	34	31

[a] Only the semivariogram of SOC stocks for grid NP2 was fitted with an exponential model; N/S – nugget to sill ratio.

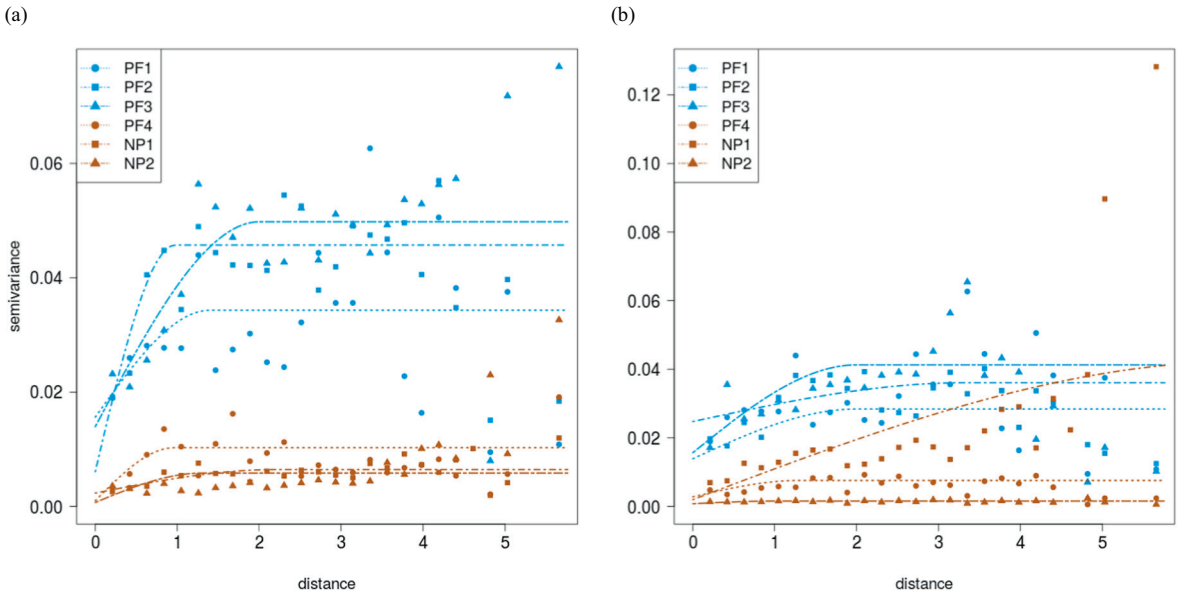

Fig. 5. The semivariograms of (a) topsoil TN stocks (kg N m^{-2}), (b) subsoil TN stocks (kg N m^{-2}), obtained for the six study grids (4 × 4 m).

Table 4
Spearman's rank correlation coefficients between SOC and total N stocks and soil factors for the six study grids, where PF1 to PF4 are grids with permafrost-affected soils and NP1 and NP2 are grids with no presence of permafrost within the upper 100 cm layer. The significant correlation coefficients are given in bold.

Parameter	Soil layer	PF1		PF2		PF3		PF4		NP1		NP2	
		SOC	N	SOC	N	SOC	N	SOC	N	SOC	N	SOC	N
AL,	Topsoil	0.09	0.15	0.08	0.06	0.08	0.11	−0.11	−0.11	NA[7]	NA	NA	NA
cm	Subsoil	0.02	0.09	−0.04	−0.07	−0.11	−0.11	−0.14	−0.18	NA	NA	NA	NA
OL,	Topsoil	−0.33	−0.30	−0.12	−0.14	−0.20	−0.18	−0.07	−0.06	0.05	0.11	−0.19	−0.12
cm	Subsoil	0.00	0.09	0.02	0.01	0.02	0.03	0.15	0.20	0.23	0.25	0.06	0.07
pH_{CaCl2}	Topsoil	0.01	0.13	**0.44**	**0.46**	0.37	0.36	0.33	0.37	0.06	0.22	−0.09	0.03
	Subsoil	−0.30	−0.34	−0.08	−0.13	0.05	0.08	−0.36	−0.34	0.22	0.38	0.03	0.28
Al_d + 0.5 Fe_d,	Topsoil	0.38	0.36	**0.48**	**0.48**	0.32	0.36	0.40	0.41	0.29	0.20	**0.46**	**0.41**
mg g^{-1}	Subsoil	0.03	0.02	−0.12	−0.10	0.00	−0.01	**0.66**	**0.65**	**0.65**	**0.68**	**0.38**	**0.55**
Cutin,	Topsoil	−0.27	−0.23	NA	NA	NA	NA	0.17	0.16	−0.18	−0.14	NA	NA
μg g^{-1}	Subsoil	−0.03	−0.02	NA	NA	NA	NA	0.16	0.14	−0.06	−0.05	NA	NA
Suberin,	Topsoil	0.06	0.05	NA	NA	NA	NA	**0.73**	**0.72**	**0.72**	**0.67**	NA	NA
μg g^{-1}	Subsoil	0.11	0.12	NA	NA	NA	NA	**0.77**	**0.73**	**0.83**	**0.83**	NA	NA
Glucose,	Topsoil	0.06	0.08	NA	NA	NA	NA	**0.69**	**0.68**	**0.63**	**0.60**	NA	NA
g kg^{-1}	Subsoil	0.01	0.05	NA	NA	NA	NA	**0.57**	**0.54**	**0.72**	**0.69**	NA	NA
TNS,	Topsoil	0.10	0.09	NA	NA	NA	NA	**0.64**	**0.63**	**0.51**	**0.47**	NA	NA
g kg^{-1}	Subsoil	0.00	0.01	NA	NA	NA	NA	**0.62**	**0.58**	**0.64**	**0.61**	NA	NA
GM/AX	Topsoil	0.20	0.19	NA	NA	NA	NA	0.11	0.11	0.05	0.00	NA	NA
ratio	Subsoil	−0.02	−0.07	NA	NA	NA	NA	0.10	0.03	−0.05	−0.06	NA	NA
RF/AX	Topsoil	−0.21	0.00	NA	NA	NA	NA	0.26	0.25	0.11	0.06	NA	NA
ratio	Subsoil	0.06	−0.01	NA	NA	NA	NA	0.07	0.05	−0.14	−0.15	NA	NA

SOC– soil organic carbon stock (kg C m^{-2}); N – total nitrogen stock (kg C m^{-2}); AL – active layer thickness; OL – organic layer thickness; Al_d + 0.5 Fe_d – dithionite-extractable pedogenic iron and aluminum hydroxides; TNS – the total neutral sugars; GM/AX ratio – the ratio of the sum of galactose C and mannose C to the sum of arabinose C and xylose C; RF/AX ratio – the ratio of the sum of rhamnose C and fucose C to the sum of arabinose C and xylose C; NA – not available (*i.e.* only grids PF1, PF4 and NP1 were measured for these parameters).

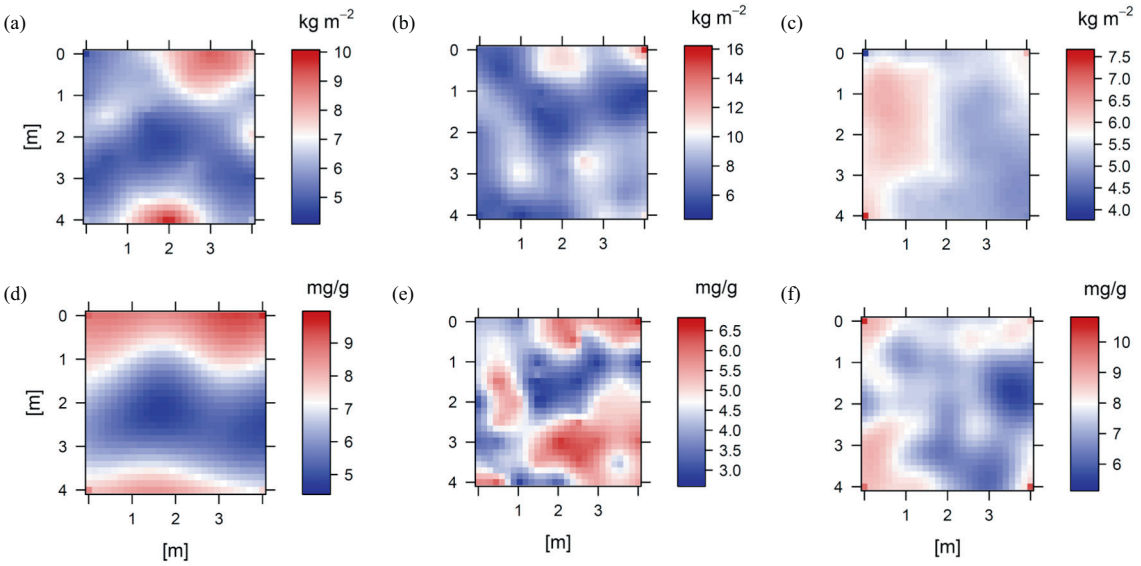

Fig. 6. The distribution maps of SOC stocks (kg C m^{-2}) and dithionite-extractable hydroxide content (0.5 Fe_d + Al_d, mg g^{-1}) in the subsoils within grids PF4 (a, d), NP1 (b, e) and NP2 (c, f), obtained using ordinary kriging.

(6.60 ± 0.27 mg g^{-1}). In contrast, in the subsoils, Al_d + 0.5 Fe_d contents within the permafrost-affected and non-permafrost grids did not differ (Table 2). Moderate, but significant ($P \leq 0.05$) positive correlations were found between the sum of Al_d + 0.5 Fe_d contents and SOC stocks as well as N stocks in the topsoils of grid PF2 and NP2 and in the subsoils of PF4 and NP1 as well as NP2 (Table 4). The results of the correlation analysis were confirmed by map comparison that indicates a moderate spatial correlation among described-above parameters in the subsoils within grids PF4, NP1 and NP2 (Fig. 6). Though, the content of pedogenic Fe and Al hydroxides in both mineral soil layers of the sites with shallow and intermediate AL showed pronounced small-scale spatial patterns that were neither spatially correlated with SOC stocks nor with any of the other measured parameters (Appendices 1–3).

3.3. Spatial relation between soil organic carbon stocks, total nitrogen stocks and plant-derived soil organic matter compounds

The content and spatial patterns of cutin- and suberin-specific monomers as well as GM/AX and RF/AX ratios in soils differed considerably within study grids PF1, PF4 and NP1, which were chosen to represent the three soil groups of various permafrost impacts for biomarker analyses. The correlations between the above-mentioned biomarkers and SOC or total N stocks in the mineral top- and subsoils were obtained using a correlation analysis (Table 4).

The content of cutin-specific monomers was significantly ($P \leq 0.05$) lower in the topsoils of site PF1 with high permafrost table (96.8 ± 9.4 μg g^{-1} dry soil) compared to the non-permafrost site NP1

Table 5
The mean values with standard errors in brackets for plant-derived soil organic matter compounds (*i.e.* cutin and suberin) and non-cellulosic neutral sugars (*i.e.* galactoce, mannose, *etc.*) as well as GM/AX and RF/AX ratios for three study grids, where PF1 (ALT = 28 cm) and PF4 (ALT = 41 cm) represented permafrost-affected soils and NP1 represents non-permafrost soils within the upper 100 cm layer. For each studied parameter, 61 samples per grid were analyzed. The different letters represent statistical differences ($P \leq 0.05$) for mean values between measured parameters for top- and subsoils among the three study grids.

Parameter	PF1				PF4				NP1			
	Topsoil		Subsoil		Topsoil		Subsoil		Topsoil		Subsoil	
Cutin, $\mu g\, g^{-1}$	96.8 (9.4)	a	44.2 (3.9)	a	148.4 (16.2)	b	43.0 (5.68)	a	135.4 (13.3)	b	45.7 (5.67)	a
Suberin, $\mu g\, g^{-1}$	101.3 (11.6)	a	49.1 (6.8)	a	101.8 (15.3)	a	79.1 (9.1)	b	110.0 (11.5)	a	77.8 (10.5)	b
Galactose, $g\, kg^{-1}$	11.8 (0.9)	a	1.9 (0.3)	a	11.3 (0.9)	a	2.1 (0.3)	a	10.5 (0.7)	a	2.0 (0.3)	a
Mannose, $g\, kg^{-1}$	11.0 (1.4)	a	2.1 (0.4)	a	10.5 (1.4)	a	1.9 (0.2)	a	9.9 (1.4)	a	1.8 (0.3)	a
Arabinose, $g\, kg^{-1}$	8.2 (0.6)	a	1.6 (0.1)	b	7.9 (0.6)	a	1.4 (0.1)	a	8.0 (0.5)	a	1.4 (0.1)	a
Xylose, $g\, kg^{-1}$	8.1 (0.6)	a	1.5 (0.1)	a	7.5 (0.5)	a	1.4 (0.1)	a	7.9 (0.6)	a	1.4 (0.1)	a
Glucose, $g\, kg^{-1}$	30.6 (2.4)	a	12.9 (1.5)	a	32.0 (2.7)	a	17.5 (1.5)	b	31.3 (2.4)	a	16.7 (1.5)	b
Ribose, $g\, kg^{-1}$	0.3 (0.0)	a	0.1 (0.0)	a	0.3 (0.0)	a	0.3 (0.1)	b	0.2 (0.0)	a	0.4 (0.1)	b
Fucose, $g\, kg^{-1}$	1.2 (0.2)	a	0.3 (0.1)	a	1.1 (0.2)	a	0.2 (0.0)	a	1.0 (0.2)	a	0.2 (0.1)	a
Rhamnose, $g\, kg^{-1}$	2.2 (0.3)	a	0.8 (0.1)	b	2.5 (0.3)	a	0.7 (0.1)	b	2.2 (0.2)	a	0.6 (0.1)	a
TNS, $g\, kg^{-1}$	73.3 (3.1)	a	21.1 (1.7)	a	73.0 (3.7)	a	25.5 (1.5)	b	71.1 (2.9)	a	24.5 (1.7)	b
GM/AX ratio	1.6 (0.2)	a	1.3 (0.2)	a	1.7 (0.3)	a	1.6 (0.2)	a	1.5 (0.2)	a	1.4 (0.2)	a
RF/AX ratio	0.2 (0.0)	a	0.4 (0.1)	a	0.3 (0.0)	a	0.4 (0.1)	a	0.2 (0.0)	a	0.3 (0.0)	a

TNS – the total neutral sugars; GM/AX ratio – the ratio of the sum of galactose C and mannose C to the sum of arabinose C and xylose C; RF/AX ratio – the ratio of the sum of rhamnose C and fucose C to the sum of arabinose C and xylose C.

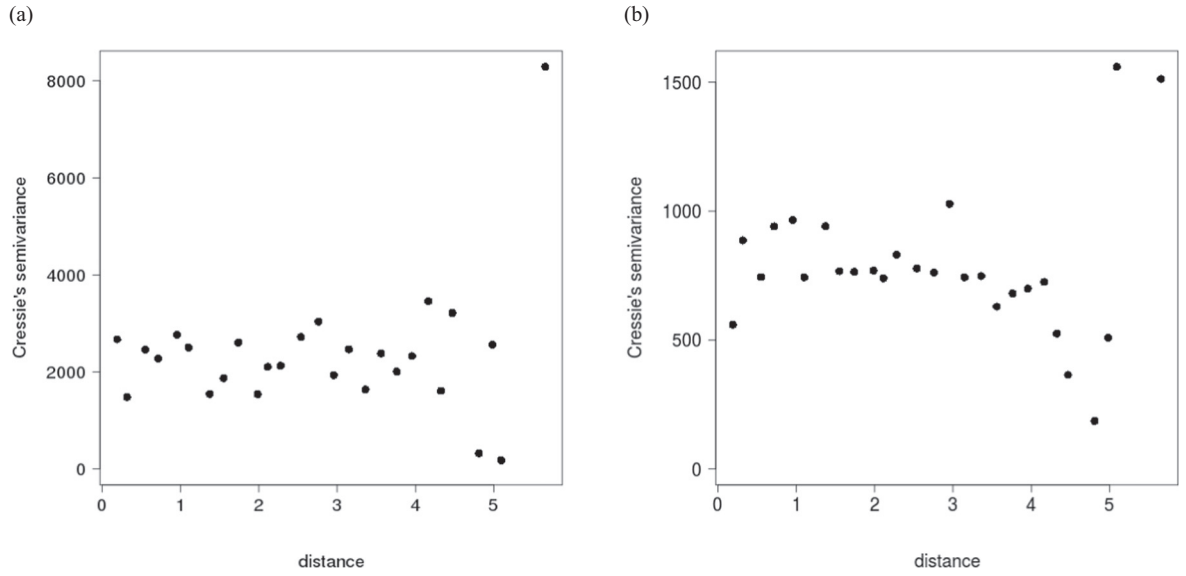

Fig. 7. The semivariograms of suberin content ($\mu g\, g^{-1}$ dry soil) in the topsoils (a) and subsoils (b) within study grid PF1.

and site PF4 with deep AL (141.9 ± 10.5 $\mu g\, g^{-1}$ dry soil) (Table 5). In the subsoils, the cutin content did not differ significantly among the three study grids and was estimated on average at 44.3 ± 2.9 $\mu g\, g^{-1}$ dry soil. Neither Spearman's rank ($P = 0.05$) nor spatial correlation was observed between the content of cutin-specific monomers and SOC stock or N stock in any mineral soil layer (Table 4). The content of suberin-specific monomers did not differ among the topsoils of the three study grids and was, on average, 104.4 ± 7.4 $\mu g\, g^{-1}$ dry soil. However, the subsoils at site PF1 were characterized by a significantly lower suberin content (49.1 ± 6.8 $\mu g\, g^{-1}$ dry soil) compared to the sites PF4 and NP1 (78.5 ± 6.9 $\mu g\, g^{-1}$ dry soil) (Table 5). The semivariogram analysis of the suberin content in both mineral soil layers at site PF1 confirmed a pure nugget effect, indicating a high degree of small-scale variability of root distribution within the upper 30 cm layer (Fig. 7). In contrast, the small-scale spatial patterns of suberin content in the top- and subsoils of grids PF4 and NP1 had strong positive correlations with SOC and N stocks, which were also confirmed by map comparison (Fig. 8a, b). One factor controlling the SOM composition in soils of different permafrost regime may be the different vegetation composition and, hence, the input of organic residues to soil. However, despite qualitative differences in plant inputs pertaining to different plant composition (Table 1, Appendix 4), the GM/AX and RF/AX ratios of the mineral soils were not significantly different in grids PF1, PF4 and NP1 and estimated on average at 1.6 and 0.3 for the topsoils and 1.5 and 0.3 for the subsoils (Table 5). The dominant plant species and plant parts at the study sites can be distinguished by their neutral sugar composition (Appendix 4). The aboveground parts of mosses (*Sphagnum* spp., *Polytrichum* spp.) were characterized by larger contribution of galactose (24–25%), mannose (26–28%), and rhamnose (8–10%) to TNS, while the content of arabinose (4–5%) and xylose (4–5%) was lower compared to aboveground parts of higher plants (Appendix 4). The sedges and horsetails (*Carex* spp., *Equisetum* spp.), shrubs (*Ledum palustre*, *Vaccinium* spp.) and the tree parts were characterized by higher contribution of arabinose (5–20%) and xylose (9–46%) to TNS and lower relative content of galactose, rhamnose and, especially mannose.

The contents of the eight specific non-cellulosic neutral sugars as well as TNS decreased with depth and were not significantly different within the three study grids (Table 5). However, significantly lower contents of ribose, glucose and TNS and significantly higher contents of arabinose in the subsoils of grid PF1 and rhamnose in the subsoils of

grid NP1 were found (Table 5). In topsoils, the contribution to TNS of the most abundant neutral sugar, glucose, accounted of about 40–42% and increased with depth, ranging in subsoils from 61% (PF1) to- 69% (PF4 and NP1). The correlation analysis showed that the "hot spots" of SOC and N stocks were related and spatially correlated to TNS in the top- and subsoils within grids PF4 and NP1 (Table 4, Fig. 8a, b). However, no significant spatial relationships were observed ($P \leq 0.05$) between SOC or N stocks and GM/AX or RF/AX ratios (Table 4).

4. Discussion

4.1. Magnitude and spatial structure of SOC and total N stocks

Significantly lower total SOC and N stocks, precisely by 32% and 38% were observed in non-permafrost grids as compared to shallow and intermediate AL soils (Table 2). The SOC and N stocks of the mineral soils (0–30 cm) underlain by permafrost at the depth of about 40 to 50 cm were about 43% and 67% higher than in non-permafrost soils, which corresponds well to a previous study at the Little Graviyka catchment (Rodionov et al., 2007). In addition, topsoil C:N ratios of the two non-permafrost soils were significantly higher, compared to the permafrost-affected soils, indicating that OC stocks may faster recover than N stocks after permafrost thaw. A recovery of SOC stocks could be a result of ongoing counterbalancing mechanisms such as the formation of reactive pedogenic minerals, organo-mineral associations and more complex soil structure as well as accelerated plant-derived OC input driven by the changes in plant community composition and increased plant productivity. Lower N stocks of non-permafrost grids compared to permafrost affected grids is most likely a result of an increasing relative contribution of root-derived OM to the overall plant-derived OM input (C:N ratio of roots is approx. 100; aboveground tissue is approx. 35 to 45) as confirmed by higher suberin contents with increasing AL thickness (Section 4.2). Moreover, lower N stocks could also be explained by increased N plant uptake, higher leaching and lateral flow rates driven by better drainage as a result of higher N availability (Nordin et al., 2004; Treat et al., 2016).

The results of geostatistical analyses demonstrated the heterogeneous spatial structure of SOC and N stocks, which is characteristic for boreal forest soils (Mishra and Riley, 2015). A moderate dependency (N/S > 25%) was also detected for SOC stocks across Alaska at the 50 and 100 m spatial scales by Mishra and Riley (2015). The Little Graviyka creek catchment was also described by Rodionov et al. (2007) as a highly heterogeneous catchment with large variations in SOC and N stocks among soil patches with different spatial positions within the landscape relief. However, a trend towards an increased homogeneity of SOC distribution in the topsoils, and N stocks in topsoils and subsoils was found with deepening of the AL in the studied ecosystem. The trend was confirmed by lower total variances and N/S ratios as well as by larger correlation lengths within sites with deeper permafrost table (PF4) and absence of permafrost (NP1, NP2) (Table 3). This finding could be explained by more homogeneous vegetation distribution and a decrease in plant biodiversity, both leading to more homogeneous spatial C input pattern at the sites with thicker AL. The N/S ratios for the studied high-latitude ecosystem in the topsoils (19–36%) and subsoils (31–52%) were comparable to N/S ratios of temperate forest soils that ranged between 20% (0–12 cm) and 55% (40–60 cm) (Schöning et al., 2006; Spielvogel et al., 2009). A number of studies in various climatic zones also confirmed that the small-scale spatial

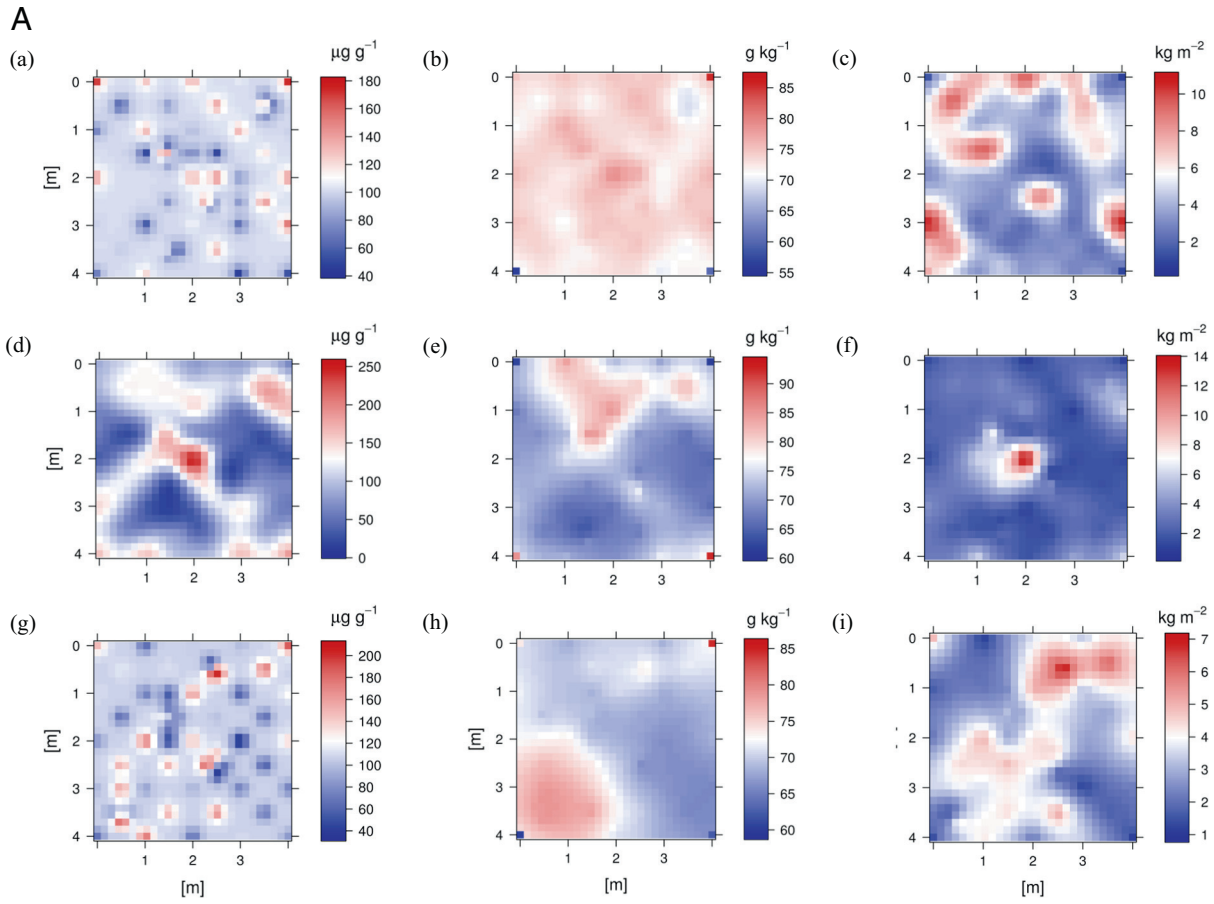

Fig. 8. a. The distribution maps of suberin (µg g^{-1} dry soil) and neutral sugar content (g kg^{-1}), and SOC stocks (kg C m^{-2}) in the topsoils of the study grids PF1 (a–c), PF4 (d–f) and NP1 (g–i), obtained using ordinary kriging.
b. The distribution maps of suberin (µg g^{-1} dry soil) and neutral sugar content (g kg^{-1}), and SOC stocks (kg C m^{-2}) in the subsoils of the study grids PF1 (a–c), PF4 (d–f) and NP1 (g–i), obtained using ordinary kriging.

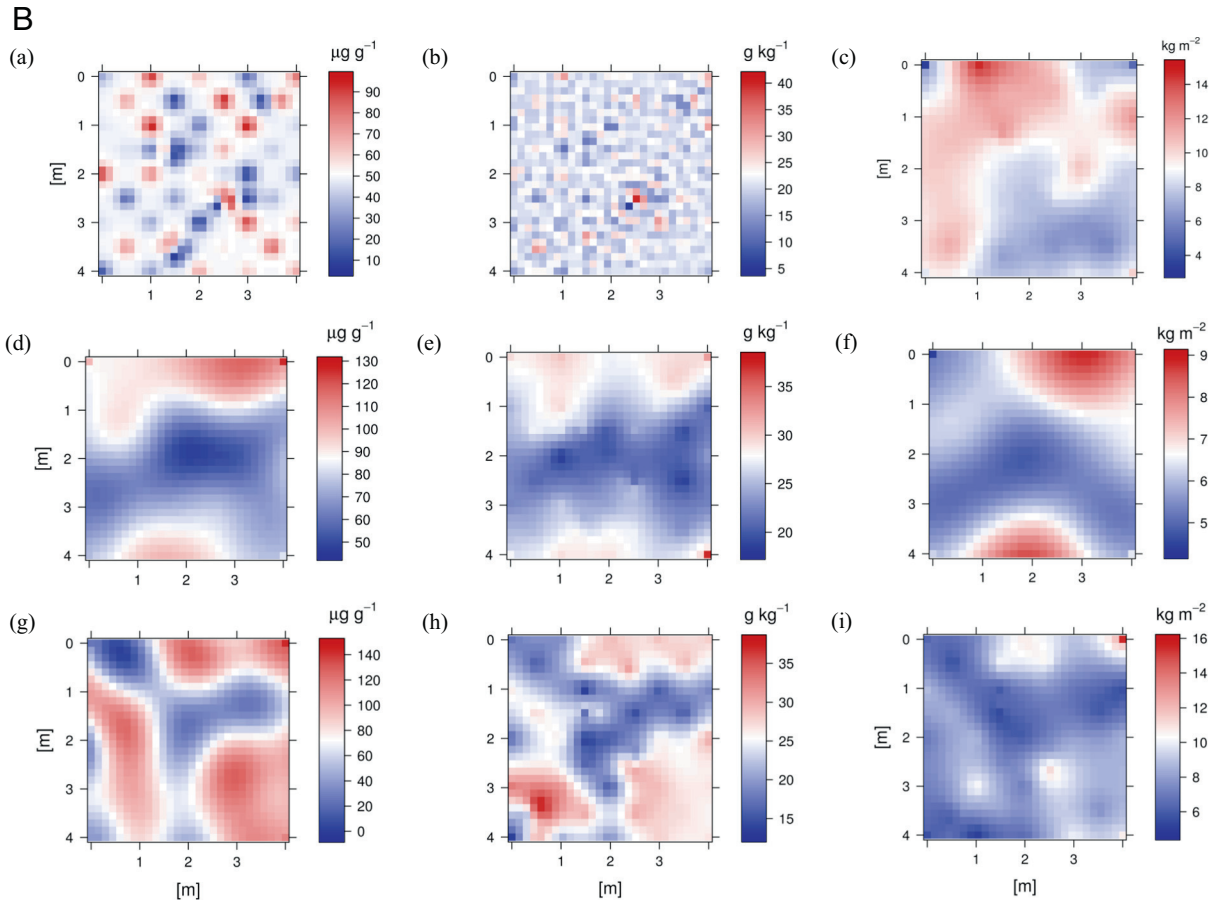

Fig. 8. (*continued*)

variability and large nugget variances of SOC stocks were typical for forest ecosystems (Liski, 1995; Paz-González et al., 2000; Schöning et al., 2006; Spielvogel et al., 2009, 2016). In order to assess the spatial patterns' changes, the range of spatial correlation of SOC and N stocks of studied mineral soils was estimated and only short-distance autocorrelation was observed from 1.46 to 1.83 m in the topsoils and from 2.44 to 3.11 m in the subsoils (Table 3). These results were in line with the correlation length for OL samples in boreal forests, between 0.77 m (Muukkonen et al., 2009) and 7.00 m (Häkkinen et al., 2011) at Scots pine (*Pinus sylvestris* L.) and Norway spruce (*Picea abies* L.) sites. The obtained results were also in agreement with autocorrelation ranges, acquired for SOC stocks in temperate forest ecosystems at Norway spruce (*Picea abies* L.) stands (Spielvogel et al., 2009, 2016) and European beech (*Fagus sylvatica* L.) sites (Schöning et al., 2006). Autocorrelation ranges for polygonal tundra ecotones are reported to be much shorter, with soil properties varying often at the decimeter to one meter scale, depending predominantly from the diameter of the periglacial geomorphological landforms such as the reticulate pattern of ice wedge polygons (Ping, 2013; Siewert, 2015). Thus, the obtained correlation length may be applicable for forest ecosystems across the globe. The relatively high small-scale spatial variability of SOC and N stocks in the studied high-latitude forest is rather a function of vegetation distribution than a result of the permafrost pattern as these variabilities are close to temperate forest soils.

4.2. Sampling design recommendations

The calculated semivariogram parameters could also be used for planning cost-efficient and adequate sampling schemes for future SOC and N inventories in high-latitude regions. The future inventories of SOM stocks in boreal forests, which would take into account high small-scale spatial variability, should be supported with a sufficient sampling design allowing the sampling distances exceed the local autocorrelation ranges (Kristensen et al., 2015; Vanguelova et al., 2016). The relative minimum detectable differences (MDDs) were calculated in order to estimate the necessary number of samples to detect a difference of 10% in the SOC and N stocks of boreal forest ecosystems. However, it was possible to calculate the MDDs only for topsoil SOC stocks for grids PF3, PF4, and N stocks for grids PF1, PF4 due to the large range, which excluded the possibility to obtain two required independent sampling sets. Calculation of MDDs for the subsoil was possible for all cases. The calculated relative MDDs have demonstrated that one would need between 500 and 700 topsoil samples within the permafrost-affected grids of 16 m^2 in order to detect a 10% difference of SOC and N stocks (Fig. 3). The required sample size was significantly smaller for the non-permafrost sites and would range between 130 and 400 samples for SOC stocks and 200 to 500 for N stocks. As the spatial variability and range of SOC stocks in this study were comparable to those estimated in temperate forest regions, the provided sample size suggestions might be applicable for other boreal and temperate forest soils. One should also note that a high variation within the study groups, the large contribution of analytical errors as well as the sampling settings (*i.e.* the distance and number of repeated samples) enlarged the recommended number of samples. Thus, similar studies across a number of additional sites and regions would be necessary in order to draw a final conclusion.

4.3. Soil parameters and organic matter sources that define the spatial patterns of soil organic carbon and total nitrogen stocks

The small-scale spatial variability of SOC and N stocks at the study grids with a deep AL (PF4) and no permafrost impact (NP1, NP2) was mostly defined by the distribution of dithionite-extractable Fe and Al hydroxides and plant-derived OC inputs (Table 4, Figs. 6, 8). The significant positive correlations between the sum of Al_d + 0.5 Fe_d and SOC or N

stocks in the subsoils at sites PF4, NP1 and NP2 (Table 4) confirmed the hypothesis that reactive secondary Al- and Fe-phases contribute to the formation of spatially distinct SOM "hot spots". The formation of these reactive pedogenic minerals as a result of ongoing weathering and increased oxic conditions associated with permafrost degradation may mitigate negative impact of permafrost on soil development in Cryosols (Zollinger et al., 2017). Using nanoscale secondary ion mass spectrometry, Mueller et al. (2017) found that the surfaces of quartz grains covered with iron oxides act as a central point of soil structure formation *via* binding with SOM and clay minerals. Furthermore, Gentsch et al. (2015b) reported that mineral-associated OM in deeper permafrost soils was up to several thousands of years old and only 1.5–5% of the mineral-associated SOC were mineralized and released as CO_2 even under favorable incubation conditions such as 60% water-holding capacity, 15 °C, and adequate nutrient supply. The above-mentioned findings emphasize that SOM could be partially stabilized *via* the formation of organo-mineral associations and microaggregates pertaining to AL deepening. This can further result in a more developed soil structure and the specific spatial distribution patters of SOM (Gentsch et al., 2015c; Gillespie, 2014; Mueller et al., 2015, 2017), similar to temperate forest soils (Kögel-Knabner et al., 2008).

Numerous studies have demonstrated the potential of cutin- and suberin-derived compounds to quantify changes of above- and belowground plant inputs in grassland and forest soils of temperate ecosystems (Mendez-Millan et al., 2010; Mueller et al., 2012; Naafs et al., 2005; Nierop, 2001; Rasse et al., 2005; Riederer et al., 1993; Spielvogel et al., 2014). The higher contribution of aboveground C inputs (*i.e.* cutin) into the topsoils of deep AL and non-permafrost sites could possibly be explained by relatively higher abundance and productivity of woody plants and understory vegetation. (Table 1; own field observations, confirmed by Filley et al., 2008). Despite the fact that especially trees have the potential to affect the local variation in soil properties through litterfall, canopy throughfall, stem flow, and shading (Chang and Matzner, 2000; Penne et al., 2010; Rothe et al., 2002; Stork and Dilly, 1998), no significant spatial correlation was observed between cutin content and SOC or N stocks (Table 4). Furthermore, the results from previous studies over the last 35 years on the spatial influence of litterfall and aboveground inputs on SOC pools and composition in forest ecosystems of different climatic zones have been ambiguous. Several studies showed that litterfall and above ground inputs influenced SOC stocks. So higher SOC and/or N stocks, and/or thicker OL were found in Podzols and Ultisols under boreal forest between 0.8 and 3 m radius from trees due to OC inputs from stem flow, bark sloughing, and/or higher needle litter input below the tree canopy (Liski, 1995; Ruark and Zarnoch, 1992). Penne et al. (2010) showed that needle litterfall was the main factor causing the spatial differences in forest floor SOC stocks in a temperate 55-year old pine stand and suggested that the heterogeneity might been controlled by stand density. Bens et al. (2006) found that OL thickness strongly depends on successional status of the forest ecosystem, reflecting the stage of the transformation from mature pine stand to beech stand. In contrast, the spatial patterns of forest floor and topsoil OC stocks of a Typic Dystrochrept and a Typic Fragiochrept (Riha et al., 1986), a Haplic Luvisol (Schöning et al., 2006), and a Leptic Cambisol (Spielvogel et al., 2009) were not observed as a function of tree distribution and leave/needle litter input. Also Hagen-Thorn et al. (2004) could not identify significant differences in C contents while comparing the litter layer under tree crowns and tree gaps in several 30 to 45-year-old pine stands. The authors explained their observations by the dominance of other environmental factors, *e.g.* small-scale topography and distribution of fallen tree stems (Spielvogel et al., 2009), patchiness of soil moisture, pH values, and N availability (Riha et al., 1986; Schöning et al., 2006), or successonal status of the forest and density of ground cover vegetation (Bens et al., 2006; Hagen-Thorn et al., 2004). All these parameters influence the spatial heterogeneity of SOM stocks and mineralization processes. Thus, it was assumed that a relatively high and continuously distributed ground cover vegetation (≈95%) within the study grids led to a homogeneous aboveground litter distribution, which could not significantly influence SOC stocks compared to the more heterogeneous distribution of belowground OC sources at the studied spatial scale. This interpretation is in line with the observations of Penne et al. (2010), who found that the spatial variability of litterfall, induced by differences in tree crown classes, increases with tree age, which may influence the vegetation cover ratio by decreasing the proportion of ground cover vegetation. Hence, taking into account that a significant proportion of old SOC is stored in permafrost soils, the spatial distribution of topsoil OC stocks would also be most likely influenced by the former aboveground vegetation patterns (*i.e.* memory effect) as well as the current stage of vegetation associations within the studied grids.

In contrast to the cutin content, the contribution of suberin to the topsoil and, especially subsoil OC was significantly higher ($P \leq 0.05$) at the "hot spots" of SOC and N accumulation within grids PF4 and NP1 in comparison to the remaining patches (Fig. 8b). Previous studies in temperate forests also specified that the spatial patterns of root-derived OM inputs contributed to the spatial variability of SOC stocks and fractions (Boettcher and Kalisz, 1990; Bugmann, 2001; Spielvogel et al., 2014, 2016; Weber and Bardgett, 2011). On the other hand, no significant correlations were found between suberin contents and SOC or N stocks for site PF1 (Table 4, Fig. 8). The root system development was most likely limited by high permafrost table at site PF1 confirmed by a rapid decrease of suberin concentrations with soil depth and densely packed root distribution (own field observations), which could also explain the pure nugget effect detected for suberin concentrations at grid PF1 (Fig. 7). The results are also in line with numerous studies showing that tundra and boreal forest ecosystems with high permafrost table exhibit very shallow rooting systems, with 80–90% of the fine roots in the top 30 cm of soil (Canadell et al., 1996; Höfle et al., 2013; Iversen et al., 2015; Jackson et al., 1996; Jobbágy and Jackson, 2000). In contrast, the majority of temperate coniferous forests allocate only about 50% of their roots in the upper 30 cm of a soil profile (Canadell et al., 1996; Jackson et al., 1996).

The obtained results indicate that root-derived OC inputs may increasingly contribute to SOM variability with AL deepening as a result of progressively differentiated rooting systems development towards the spatially heterogeneous and niche specific root distribution in temperate forests. This development results in intensively rooted patches, "hot spots" of SOM stocks, rich in suberin-derived lipids, root exudates, and root-debris. The formation of SOM in such "hot spots" is likely dominated by the accumulation of OM derived from the decomposition of root inputs, which might have a low degree of stabilization, and exceed OM accumulated through aboveground litterfall (Träger et al., 2017). At the same time, SOM formation in neighboring patches, with lower belowground OC inputs, might be dominated by other processes, *e.g.* leaching of dissolved OM from the forest floor and adsorption and/or (co-)precipitation processes with the mineral phase.

Furthermore, the "hot spots" of SOC and N stocks in the topsoil and subsoils of grids PF4 and NP1 were spatially correlated with high TNS contents (Table 4, Fig. 8a, b). The enrichment of TNS within high suberin content patches could possibly be explained by a larger contribution of TNS-C to the total C content for the roots compared to twigs and foliage of all studied tree species (Appendix 4). The plant roots may also considerably contribute to TNS content by the continuous recycling of organic substances and biosynthesis of sugars by microbes in the rhizosphere (Derrien et al., 2007). Higher microbial abundance and diversity as well as faster microbial growth occur in rhizosphere soil compared to root-free soil (Berg and Smalla, 2009; Paterson et al., 2007). While the overall TNS content was spatially correlated with SOC and N stocks in grids PF4 and NP1, we could not observe the spatial relationship between SOC or N stocks and TNS composition (*e.g.* GM/AX or RF/AX ratio) (Table 4). According to traditional concepts, the relative contribution of plant-derived *vs.* microbial-derived neutral sugars to SOM is estimated by calculation of molar ratios of the sugar monomers (G + M)/(A + X) (Oades, 1984) or (R + F)/(A + X) (Murayama, 1984). However, large differences in GM/AX and RF/AX ratios among dominant plant species were observed at the study grids (Appendix 4). The moss species were characterized by large GM/AX (> 5) and RF/AX ratios (> 1) thus, their tissues would have been

erroneously considered as microbial-derived based on Oades' concept (Oades et al., 1984). These results are in accordance with previous studies, where galactose, rhamnose, and mannose were identified as indicators of numerous of mosses species (*e.g.* for *Sphagnum* and *Polytrichum* spp. – Comont et al., 2006; Nierop, 2001; Popper and Fry, 2003; for *Scleropodium purum*, *Thuidium tamariscinum*, *Rhytidiadelphus triquetrus* – Prietzel et al., 2013; Dao et al., 2018). Therefore, it was assumed that the mixed signature of microbial neutral sugars and the neutral sugar input from a notable portion of mosses in the understory vegetation of the studied patches resulted in unspecific GM/AX and RF/AX patterns that cannot be assigned to a distinct source and are, therefore, not spatially correlated to any other soil properties.

5. Conclusion

Although an overall trend towards lower SOC and N stocks was observed with deeper permafrost table, the C sequestration potential of high-latitude permafrost soils, especially within the discontinuous permafrost zone, could improve gradually in the long term. The ongoing pedogenesis in the thawed layers characterized by enlarged incorporation of above- and especially belowground plant residues into SOM, and formation of organo-mineral associations and soil structure development could potentially counterbalance C losses driven by permafrost degradation as long-term impact of ongoing global change. However, the pedogenic destabilization processes such as permafrost thaw and associated decomposition of SOM are relatively faster in comparison to the stabilization processes, *e.g.* the effective stabilization in soil aggregates, organo-mineral complexes formation, and development of a deep root system as plant-derived SOC source in the "newly" thawed soil depths. The losses of C and N were highest for OL and topsoils within the study catchment. Likewise, the importance of mineral soil for SOM stabilization was confirmed by relatively higher contribution of the subsoils (44%) to the total SOC stocks, associated with increased root-derived C inputs and higher amounts of iron and aluminum hydroxides as the centers of aggregate formation.

The spatial heterogeneity and "hot spots" of SOC and N stocks in high-latitude forest soils with deep AL were mostly defined by belowground (*i.e.* suberin) plant-derived OC inputs and the availability of pedogenic reactive mineral surfaces at the small scale. This confirms the significance of the spatial structure in order to understand SOM degradation and stabilization processes as well as to estimate and improve soil mapping and environmental models. This is of particular importance for the carbon-climate feedback prediction by quantifying SOC and N stocks of discontinuous permafrost regions. The recommendations on required amount of samples for mineral soil with various permafrost impacts could assist in the estimations of SOC and N stocks and prediction of potential C and N losses across the cold-climate regions.

Acknowledgments

Financial support was provided by the German Research Foundation (Deutsche Forschungsgemeinschaft, DFG, Sa2521/1-1 and SP943/2-1). Olga Shibistova and Georg Guggenberger appreciate funding from the Russian Ministry of Education and Science (no. 14.B25.31.0031). The authors would like to thank the Igarka Geocryological Laboratory (Russian Federation) and, especially A.I. Pimov for his excellent technical assistance. Many thanks to Ulli Bange and Brigitte Mann (University of Koblenz-Landau, Germany) for assistance in laboratory measurements and to Jan Obermeier (Georg-August-University of Goettingen) for measuring and helping in identifying cutin- and suberin-derived lipid monomers.

Appendix 1. The distribution maps of SOC stocks (kg C m^{-2}) and dithionite soluble hydroxide content (Al_d + 0.5 Fe_d, mg g^{-1}) in the topsoils within grids PF1 (a, d), PF2 (b, e) and PF3 (c, f), obtained using ordinary kriging

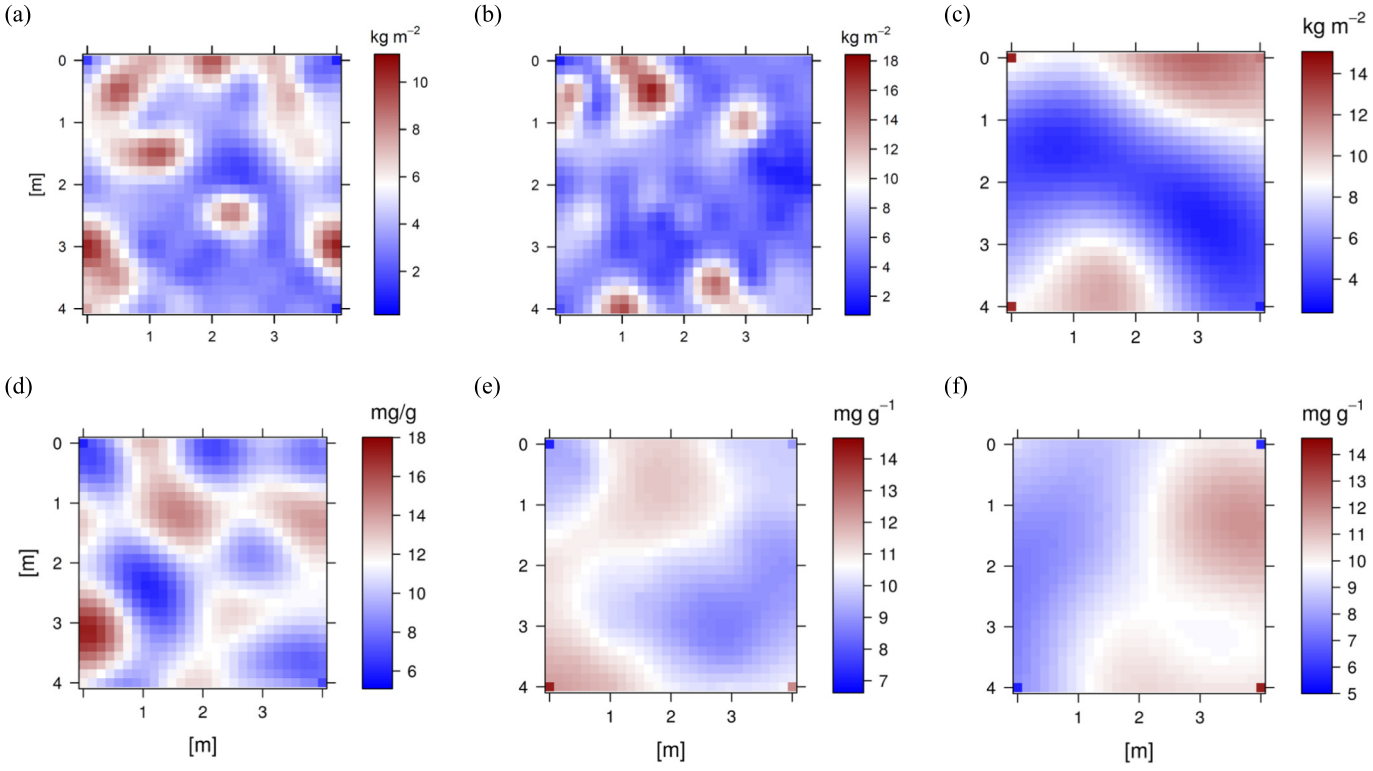

Appendix 2. The distribution maps of SOC stocks (kg C m^{-2}) and dithionite soluble hydroxide content (Al_d + 0.5 Fe_d, mg g^{-1}) in the subsoils within grids PF1 (a, d), PF2 (b, e) and PF3 (c, f), obtained using ordinary kriging

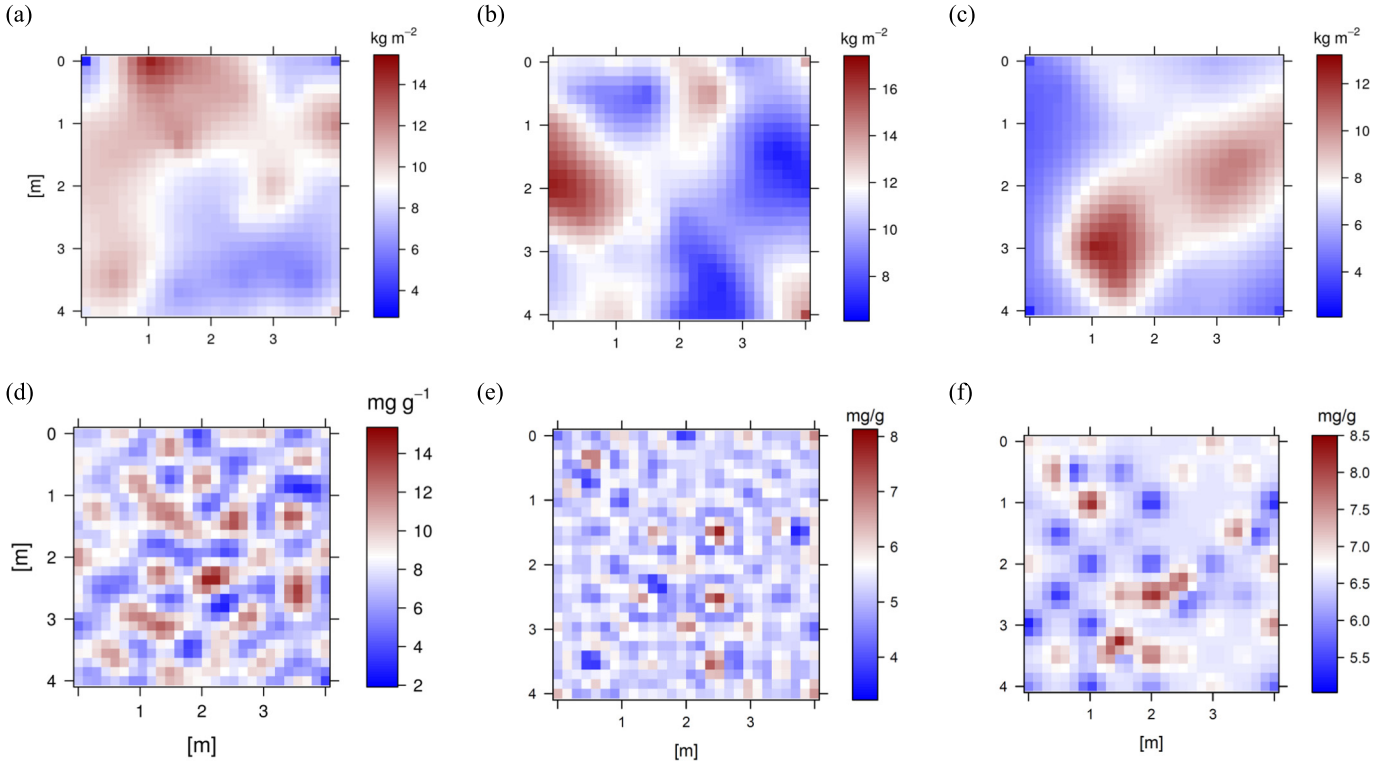

Appendix 3. The distribution maps of SOC stocks (kg C m^{-2}) and dithionite soluble hydroxide content pedogenic hydroxide content (Al_d + 0.5 Fe_d, mg g^{-1}) in the topsoils within grids PF4 (a, d), NP1 (b, e) and NP2 (c, f), obtained using ordinary kriging

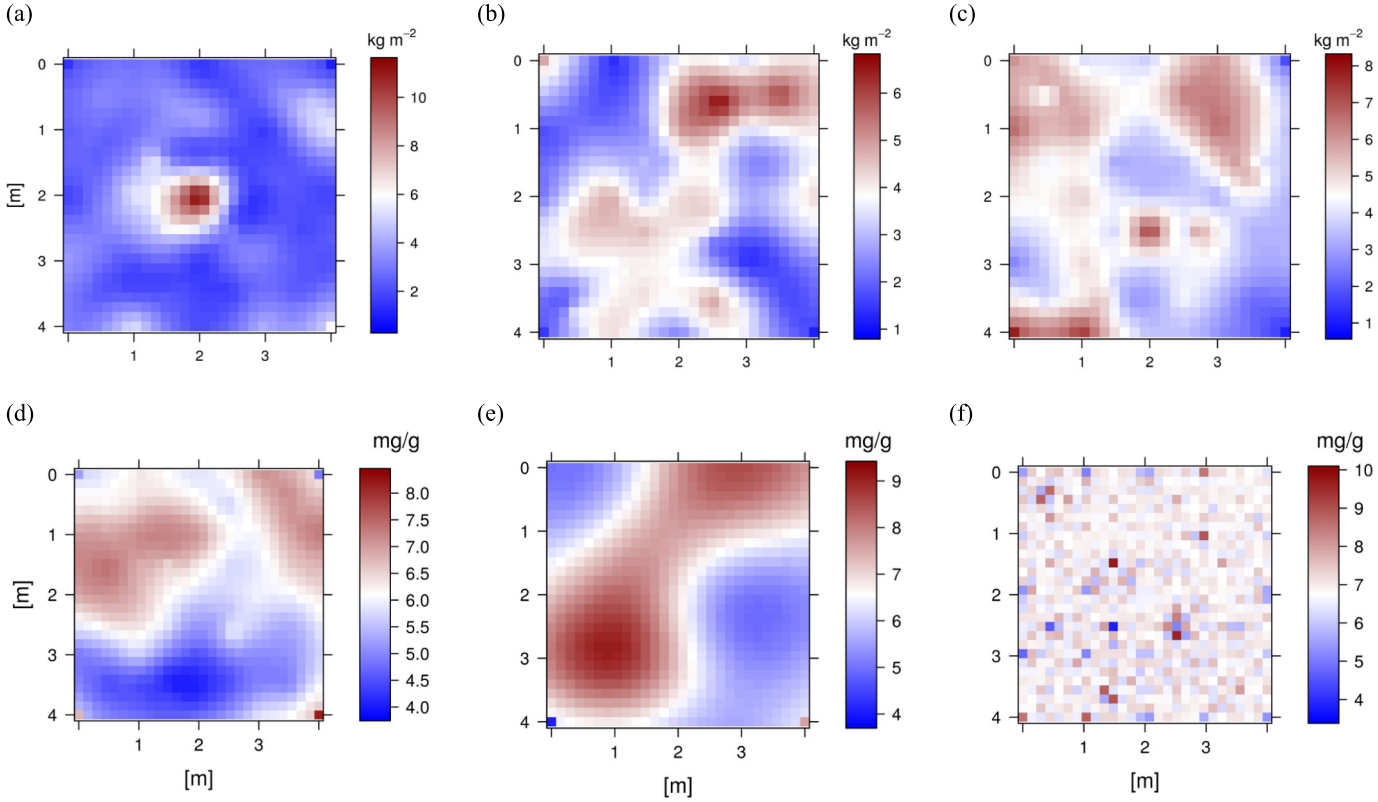

Appendix 4. The concentrations of different non-cellulosic polysaccharide monomers and mass ratios of (galactose + mannose) / (arabinose + xylose) and (rhamnose + fucose) / (arbinose + xylose) for important plant species sampled at the study grids

	Plant species	Plant part	Glucose	Rhamnose	Fucose	Ribose	Galactose	Mannose	Arabinose	Xylose	GM/AX	RF/AX	ΣNS
			g kg^{-1} OC										
Tree species	*Picea*	Needles	53,6	2,8	1,4	0,2	15,1	29,2	24.6	14.1	1.14	0.11	141.1
	obovata	Twigs	45.0	3.0	1.3	0.2	28.1	22.0	19.2	14.4	1.5	0.13	133.2
	Ledeb	Roots	133.8	3.3	1.0	0.1	27.0	38.8	15.4	21.8	1.77	0.12	241.3
	Larix sibirica	Needles	65.7	3.4	1.2	0.1	26.0	28.5	17.0	14.6	1.73	0.14	156.6
	Ledeb.	Twigs	45.2	1.2	0.8	0.2	24.2	22.2	18.2	11.7	1.55	0.07	123.7
		Roots	123.7	1.8	0.5	0.3	14.0	39.5	17.1	21.3	1.39	0.06	218.2
	Betula	Leaves	18.5	4.4	0.5	0.2	16.5	2.4	14.8	43.6	0.32	0.08	100.8
	pendula	Twigs	44.8	4.6	0.5	0.1	11.1	2.3	16.7	53.2	0.19	0.07	133.1
	Roth.	Roots	51.5	4.1	0.7	0.1	15.6	6.4	16.0	61.6	0.28	0.06	156.1
	Betual nana	Leaves	16.9	4.6	0.3	0.3	15.2	2.3	15.3	38.5	0.33	0.09	93.4
	L.	Twigs	47.0	5.6	0.6	0.1	12.0	2.0	12.0	37.6	0.28	0.12	116.9
		Roots	54.3	4.1	0.5	0.2	13.4	5.5	14.6	58.8	0.26	0.06	151.4
Understory and ground cover	*Ledum*	AG	45.0	2.9	0.6	0.3	20.4	4.6	12.4	32.3	0.56	0.08	118.5
	palustre L.	Roots	81.2	3.0	0.3	0.1	28.0	5.3	9.2	71.3	0.41	0.04	198.4
	Vaccinium	AG	47.1	2.9	0.6	0	18.7	4.7	11.0	39.5	0.46	0.07	124.6
	spp.	Roots	87.5	2.5	0.4	0.1	26.9	6.5	9.0	65.3	0.45	0.04	198.3
	Sphagnum spp.	AG	61.3	20.0	1.2	0.2	47.8	51.9	11.0	8.2	5.2	1.11	201.5
	Polytrichum spp.	AG	67.0	18.8	1.5	0	56.2	62.1	9.1	10.1	6.14	1.06	224.9
	Equisetum spp.	AG	50.2	1.7	0.4	0.2	20.8	4.6	38.5	100.4	0.18	0.02	216.8
	Carex spp.	AG	49.1	1.8	0.7	0.2	20.2	3.4	41.3	89.9	0.18	0.02	206.5

ΣNS – the sum of neutral sugar concentrations; AG – aboveground plant material.

References

Banfield, G.E., Bhatti, J.S., Jiang, H., Apps, M.J., 2002. Variability in regional scale estimates of carbon stocks in boreal forest ecosystems: results from West-Central Alberta. For. Ecol. Manag. 169, 15–27. http://dx.doi.org/10.1016/S0378-1127(02)00292-X.

Baritz, R., Eberhardt, E., Van Liedekerke, M.H., Panagos, P., 2008. Environmental Assessment of Soil for Monitoring Volume III: Database Design and Selection. http://dx.doi.org/10.2788/93697.

Baumann, F., He, J.S., Schmidt, K., Kühn, P., Scholten, T., 2009. Pedogenesis, permafrost, and soil moisture as controlling factors for soil nitrogen and carbon contents across the Tibetan Plateau. Glob. Chang. Biol. 15, 3001–3017. http://dx.doi.org/10.1111/j.1365-2486.2009.01953.x.

Beermann, F., Langer, M., Wetterich, S., Strauss, J., Boike, J., Schirrmeister, L., Pfeiffer, E., Kutzbach, L., 2016. Permafrost thaw and release of inorganic nitrogen from polygonal tundra soils in eastern Siberia. Biogeosci. Discuss. 1–27. http://dx.doi.org/10.5194/bg-2016-117.

Bens, O., Buczko, U., Sieber, S., Hüttl, R.F., 2006. Spatial variability of O layer thickness and humus forms under different pine beech-forest transformation stages in NE Germany. J. Plant Nutr. Soil Sci. 169, 5–15. http://dx.doi.org/10.1002/jpln.200521734.

Berg, G., Smalla, K., 2009. Plant species and soil type cooperatively shape the structure and function of microbial communities in the rhizosphere. FEMS Microbiol. Ecol. http://dx.doi.org/10.1111/j.1574-6941.2009.00654.x.

Bischoff, J., Sparkes, R.B., Selver, A.D., Spencer, R.G.M., Gustafsson, Ö., Semiletov, I.P., Dudarev, O.V., Wagner, D., Rivkina, E., Van Dongen, B.E., Talbot, H.M., 2016. Source, transport and fate of soil organic matter inferred from microbial biomarker lipids on the East Siberian Arctic Shelf. Biogeosciences 13, 4899–4914. http://dx.doi.org/10.5194/bg-13-4899-2016.

Bockheim, J.G., Hinkel, K.M., 2007. The importance of "deep" organic carbon in permafrost-affected soils of arctic Alaska. Soil Sci. Soc. Am. J. 71, 1889. http://dx.doi.org/10.2136/sssaj2007.0070N.

Boettcher, S.E., Kalisz, P.J., 1990. Single-tree influence on soil properties in the mountains of eastern Kentucky. Ecology. http://dx.doi.org/10.2307/1938273.

Buckeridge, K.M., Schaeffer, S.M., Schimel, J.P., 2016. Vegetation leachate during arctic thaw enhances soil microbial phosphorus. Ecosystems 19, 477–489. http://dx.doi.org/10.1007/s10021-015-9947-9.

Bugmann, H., 2001. A review of forest gap models. Clim. Chang. http://dx.doi.org/10.1023/A:1012525626267.

Canadell, J., Jackson, R.B., Ehleringer, J.B., Mooney, H.A., Sala, O.E., Schulze, E.-D., 1996. Maximum rooting depth of vegetation types at the global scale. Oecologia 108, 583–595. http://dx.doi.org/10.1007/BF00329030.

Chang, S.C., Matzner, E., 2000. The effect of beech stemflow on spatial patterns of soil solution chemistry and seepage fluxes in a mixed beech/oak stand. Hydrol. Process. 14, 135–144. http://dx.doi.org/10.1002/(SICI)1099-1085(200001)14:1<135::AID-HYP915>3.0.CO;2-R.

Comont, L., Laggoun-Défarge, F., Disnar, J.R., 2006. Evolution of organic matter indicators in response to major environmental changes: the case of a formerly cut-over peat bog (Le Russey, Jura Mountains, France). Org. Geochem. 37, 1736–1751. http://dx.doi.org/10.1016/j.orggeochem.2006.08.005.

Dao, T.T., Gentsch, N., Mikutta, R., Sauheitl, L., Shibistova, O., Wild, B., Schnecker, J., Bárta, J., Čapek, P., Gittel, A., Lashchinskiy, N., Urich, T., Šantrůčková, H., Richter, A., Guggenberger, G., 2018. Fate of carbohydrates and lignin in north-east Siberian permafrost soils. Soil Biol. Biochem. 116, 311–322. http://dx.doi.org/10.1016/j.soilbio.2017.10.032.

Delarue, F., Laggoun-Défarge, F., Disnar, J.R., Lottier, N., Gogo, S., 2011. Organic matter sources and decay assessment in a *Sphagnum*-dominated peatland (Le Forbonnet, Jura Mountains, France): impact of moisture conditions. Biogeochemistry 106, 39–52. http://dx.doi.org/10.1007/s10533-010-9410-0.

Deng, J., Gu, Y., Zhang, J., Xue, K., Qin, Y., Yuan, M., Yin, H., He, Z., Wu, L., Schuur, E.A.G., Tiedje, J.M., Zhou, J., 2015. Shifts of tundra bacterial and archaeal communities along a permafrost thaw gradient in Alaska. Mol. Ecol. 24, 222–234. http://dx.doi.org/10.1111/mec.13015.

Derrien, D., Marol, C., Balesdent, J., 2007. Microbial biosyntheses of individual neutral sugars among sets of substrates and soils. Geoderma 139, 190–198. http://dx.doi.org/10.1016/j.geoderma.2007.01.017.

Diggle, P.J., 2008. Model-based geostatistics by Diggle, P. J. and Ribeiro, P. J. Biometrics 64, 653–654. http://dx.doi.org/10.1111/j.1541-0420.2008.01026_3.x.

Eder, E., Spielvogel, S., Kölbl, A., Albert, G., Kögel-Knabner, I., 2010. Analysis of hydrolysable neutral sugars in mineral soils: improvement of alditol acetylation for gas chromatographic separation and measurement. Org. Geochem. 41, 580–585. http://dx.doi.org/10.1016/j.orggeochem.2010.02.009.

Filley, T.R., Boutton, T.W., Liao, J.D., Jastrow, J.D., Gamblin, D.E., 2008. Chemical changes to nonaggregated particulate soil organic matter following grassland-to-woodland transition in a subtropical savanna. J. Geophys. Res. 113. http://dx.doi.org/10.1029/2007jg000564.

Finger, R.A., Turetsky, M.R., Kielland, K., Ruess, R.W., Mack, M.C., Euskirchen, E.S., 2016. Effects of permafrost thaw on nitrogen availability and plant-soil interactions in a boreal Alaskan lowland. J. Ecol. http://dx.doi.org/10.1111/1365-2745.12639.

Finke, P.A., Bierkens, M.F., De Willigen, P., 2002. Choosing appropriate upscaling and downscaling methods for environmental research. Int. Assoc. Hydrol. Sci. 405–409.
Flessa, H., Rodionov, A., Guggenberger, G., Fuchs, H., Magdon, P., Shibistova, O., Zrazhevskaya, G., Mikheyeva, N., Kasansky, O., Blodau, C., 2008. Landscape controls of CH4 fluxes in a catchment of the forest tundra ecotone in northern Siberia. Glob. Chang. Biol. 14, 2040–2056. http://dx.doi.org/10.1111/j.1365-2486.2008.01633.x.
Fuchs, H., Magdon, P., Kleinn, C., Flessa, H., 2009. Estimating aboveground carbon in a catchment of the Siberian forest tundra: combining satellite imagery and field inventory. Remote Sens. Environ. 113, 518–531. http://dx.doi.org/10.1016/j.rse.2008.07.017.
Gentsch, N., Mikutta, R., Alves, R.J.E., Barta, J., Čapek, P., Gittel, A., Hugelius, G., Kuhry, P., Lashchinskiy, N., Palmtag, J., Richter, A., Šantrůčková, H., Schnecker, J., Shibistova, O., Urich, T., Wild, B., Guggenberger, G., 2015a. Storage and transformation of organic matter fractions in cryoturbated permafrost soils across the Siberian Arctic. Biogeosciences 12, 4525–4542. http://dx.doi.org/10.5194/bg-12-4525-2015.
Gentsch, N., Mikutta, R., Alves, R.J.E., Barta, J., Čapek, P., Gittel, A., Hugelius, G., Kuhry, P., Lashchinskiy, N., Palmtag, J., Richter, A., Šantrůčková, H., Schnecker, J., Shibistova, O., Urich, T., Wild, B., Guggenberger, G., 2015b. Storage and transformation of organic matter fractions in cryoturbated permafrost soils across the Siberian Arctic. Biogeosciences 12, 4525–4542. http://dx.doi.org/10.5194/bg-12-4525-2015.
Gentsch, N., Mikutta, R., Shibistova, O., Wild, B., Schnecker, J., Richter, A., Urich, T., Gittel, A., Šantrůčková, H., Bárta, J., Lashchinskiy, N., Mueller, C.W., Fuß, R., Guggenberger, G., 2015c. Properties and bioavailability of particulate and mineral-associated organic matter in Arctic permafrost soils, Lower Kolyma Region, Russia. Eur. J. Soil Sci. http://dx.doi.org/10.1111/ejss.12269. (n/a-n/a).
Gillespie, A.W., 2014. Perennially and Annually Frozen Soil Carbon Differ in Their Susceptibility to Decomposition: Analysis of Subarctic Earth Hummocks by Bioassay, XANES and Pyrolysis. pp. 77–79. http://dx.doi.org/10.1016/j.soilbio.2013.09.021.
Guggenberger, G., Rodionov, A., Grabe, M., Kasansky, O.A., 2006. The Contribution of Black Carbon to the Carbon Storage in a Permafrost Ecosystem. pp. 75–84.
Guggenberger, G., Rodionov, A., Shibistova, O., Grabe, M., Kasansky, O.A., Fuchs, H., Mikheyeva, N., Zrazhevskaya, G., Flessa, H., 2008. Storage and mobility of black carbon in permafrost soils of the forest tundra ecotone in Northern Siberia. Glob. Chang. Biol. 14, 1367–1381. http://dx.doi.org/10.1111/j.1365-2486.2008.01568.x.
Gundelwein, A., Müller-Lupp, T., Sommerkorn, M., Haupt, E.T.K., Pfeiffer, E.M., Wiechmann, H., 2007. Carbon in tundra soils in the Lake Labaz region of arctic Siberia. Eur. J. Soil Sci. 58, 1164–1174. http://dx.doi.org/10.1111/j.1365-2389.2007.00908.x.
Hagen-Thorn, A., Callesen, I., Armolaitis, K., Nihlgård, B., 2004. The impact of six European tree species on the chemistry of mineral topsoil in forest plantations on former agricultural land. For. Ecol. Manag. 195, 373–384. http://dx.doi.org/10.1016/j.foreco.2004.02.036.
Häkkinen, M., Heikkinen, J., Mäkipää, R., 2011. Soil carbon stock increases in the organic layer of boreal middle-aged stands. Biogeosciences 8, 1279–1289. http://dx.doi.org/10.5194/bg-8-1279-2011.
Harms, T.K., Edmonds, J.W., Genet, H., Creed, I.F., Aldred, D., Balser, A., Jones, J.B., 2016. Catchment influence on nitrate and dissolved organic matter in Alaskan streams across a latitudinal gradient. J. Geophys. Res. G: Biogeosci. 121, 350–369. http://dx.doi.org/10.1002/2015JG003201.
Harris, D., Horwáth, W.R., van Kessel, C., 2001. Acid fumigation of soils to remove carbonates prior to total organic carbon or CARBON-13 isotopic analysis. Soil Sci. Soc. Am. J. 65, 1853. http://dx.doi.org/10.2136/sssaj2001.1853.
Hatfield, J.L., 2001. Upscaling and downscaling methods for environmental research. J. Environ. Qual. 30, 1100. http://dx.doi.org/10.2134/jeq2001.3031100x.
Hedges, J.I., Stern, J.H., 1984. Carbon and nitrogen determinations of carbonate-containing solids. Limnol. Oceanogr. 29, 657–663. http://dx.doi.org/10.4319/lo.1984.29.3.0657.
Hobbie, S.E., Schimel, J.P., Trumbore, S.E., Randerson, J.R., 2000. Controls over carbon storage and turnover in high-latitude soils. Glob. Chang. Biol. 6, 196–210. http://dx.doi.org/10.1046/j.1365-2486.2000.06021.x.
Hoffmann, U., Hoffmann, T., Jurasinski, G., Glatzel, S., Kuhn, N.J., 2014. Assessing the spatial variability of soil organic carbon stocks in an alpine setting (Grindelwald, Swiss Alps). Geoderma 232–234, 270–283. http://dx.doi.org/10.1016/j.geoderma.2014.04.038.
Höfle, S., Rethemeyer, J., Mueller, C.W., John, S., 2013. Organic matter composition and stabilization in a polygonal tundra soil of the Lena Delta. Biogeosciences 10, 3145–3158. http://dx.doi.org/10.5194/bg-10-3145-2013.
Holmgren, G.G.S., 1967. A Rapid Citrate-dithionite Extractable Iron Procedure. 1. pp. 7–8. http://dx.doi.org/10.2136/sssaj1967.03615995003100020020x.
Hugelius, G., 2012. Spatial upscaling using thematic maps: an analysis of uncertainties in permafrost soil carbon estimates. Glob. Biogeochem. Cycles 26, 2011–2012. http://dx.doi.org/10.1029/2011GB004154.
Hugelius, G., Virtanen, T., Kaverin, D., Pastukhov, A., Rivkin, F., Marchenko, S., Romanovsky, V., Kuhry, P., 2011. High-resolution mapping of ecosystem carbon storage and potential effects of permafrost thaw in periglacial terrain, European Russian Arctic. J. Geophys. Res. Biogeosci. 116, 1–14. http://dx.doi.org/10.1029/2010JG001606.
Hugelius, G., Strauss, J., Zubrzycki, S., Harden, J.W., Schuur, E.A.G., Ping, C.L., Schirrmeister, L., Grosse, G., Michaelson, G.J., Koven, C.D., O'Donnell, J.A., Elberling, B., Mishra, U., Camill, P., Yu, Z., Palmtag, J., Kuhry, P., 2014. Estimated stocks of circumpolar permafrost carbon with quantified uncertainty ranges and identified data gaps. Biogeosciences 11, 6573–6593. http://dx.doi.org/10.5194/bg-11-6573-2014.
IPCC, 2000. Land Use, Land-Use Change, and Forestry. Forestry. pp. 1–9. http://dx.doi.org/10.2277/0521800838.
IPCC, 2007. IPCC Fourth Assessment Report (AR4). Ipcc 1, 976. doi:ISSN: 02767783.
IUSS Working Group WRB, 2014. World reference base for soil resources 2014. International soil classification system for naming soils and creating legends for soil maps. In: World Soil Resources Reports No. 106, http://dx.doi.org/10.1017/S0014479706394902.
Iversen, C.M., Sloan, V.L., Sullivan, P.F., Euskirchen, E.S., Mcguire, A.D., Norby, R.J., Walker, A.P., Warren, J.M., Wullschleger, S.D., 2015. The unseen iceberg: plant roots in arctic tundra. New Phytol. http://dx.doi.org/10.1111/nph.13003.
Jackson, R.B., Canadell, J., Ehleringer, J.R., Mooney, H.A., Sala, O.E., Schulze, E.D., 1996. A global analysis of root distributions for terrestrial biomes. Oecologia 108, 389–411. http://dx.doi.org/10.1007/BF00333714.
Jobbágy, E.G., Jackson, R.B., 2000. The vertical distribution of soil organic carbon and its relation to climate and vegetation. Ecol. Appl. 10, 423–436. http://dx.doi.org/10.2307/2641104.
Kawahigashi, M., Kaiser, K., Rodionov, A., Guggenberger, G., 2006. Sorption of dissolved organic matter by mineral soils of the Siberian forest tundra. Glob. Chang. Biol. 12, 1868–1877. http://dx.doi.org/10.1111/j.1365-2486.2006.01203.x.
Köchy, M., Hiederer, R., Freibauer, A., 2015. Global distribution of soil organic carbon – part 1: masses and frequency distributions of SOC stocks for the tropics, permafrost regions, wetlands, and the world. Soil 1, 351–365. http://dx.doi.org/10.5194/soil-1-351-2015.
Kögel-Knabner, I., Guggenberger, G., Kleber, M., Kandeler, E., Kalbitz, K., Scheu, S., Eusterhues, K., Leinweber, P., 2008. Organo-mineral associations in temperate soils: integrating biology, mineralogy, and organic matter chemistry. J. Plant Nutr. Soil Sci. 171, 61–82. http://dx.doi.org/10.1002/jpln.200700048.
Krasilnikov, P., Carre, F., Montanarella, L., 2008. Soil geography and geostatistics concepts and applications. Soil Sci. http://dx.doi.org/10.1016/j.coi.2010.10.007.
Kristensen, T., Ohlson, M., Bolstad, P., Nagy, Z., 2015. Spatial variability of organic layer thickness and carbon stocks in mature boreal forest stands—implications and suggestions for sampling designs. Environ. Monit. Assess. 187. http://dx.doi.org/10.1007/s10661-015-4741-x.
Kutzbach, L., Wagner, D., Pfeiffer, E.M., 2004. Effect of microrelief and vegetation on methane emission from wet polygonal tundra, Lena Delta, Northern Siberia. Biogeochemistry 69, 341–362. http://dx.doi.org/10.1023/B:BIOG.0000031053.81520.db.
Lal, R., 2009. Challenges and opportunities in soil organic matter research. Eur. J. Soil Sci. 60, 158–169. http://dx.doi.org/10.1111/j.1365-2389.2008.01114.x.
Lawrence, D.M., Koven, C.D., Swenson, S.C., Riley, W.J., Slater, A.G., 2015. Permafrost thaw and resulting soil moisture changes regulate projected high-latitude CO 2 and CH 4 emissions. Environ. Res. Lett. 10, 94011. http://dx.doi.org/10.1088/1748-9326/10/9/094011.
Lipson, D.A., Raab, T.K., Parker, M., Kelley, S.T., Brislawn, C.J., Jansson, J., 2015. Changes in microbial communities along redox gradients in polygonized Arctic wet tundra soils. Environ. Microbiol. Rep. 7, 649–657. http://dx.doi.org/10.1111/1758-2229.12301.
Liski, J., 1995. Variation in Soil Organic Carbon and Thickness of Soil Horizons within a Boreal Forest Stand - Effect of Trees and Implications for Sampling. Silva Fenn. doi:S
Loranty, M.M., Lieberman-Cribbin, W., Berner, L.T., Natali, S.M., Goetz, S.J., Alexander, H.D., Kholodov, A.L., 2016. Spatial variation in vegetation productivity trends, fire disturbance, and soil carbon across arctic-boreal permafrost ecosystems. Environ. Res. Lett. 11, 95008. http://dx.doi.org/10.1088/1748-9326/11/9/095008.
Mendez-Millan, M., Dignac, M.F., Rumpel, C., Rasse, D.P., Derenne, S., 2010. Molecular dynamics of shoot vs. root biomarkers in an agricultural soil estimated by natural abundance 13C labelling. Soil Biol. Biochem. 42, 169–177. http://dx.doi.org/10.1016/j.soilbio.2009.10.010.
Mishra, U., Riley, W.J., 2012. Alaskan soil carbon stocks: spatial variability and dependence on environmental factors. Biogeosciences 9, 3637–3645. http://dx.doi.org/10.5194/bg-9-3637-2012.
Mishra, U., Riley, W.J., 2015. Scaling impacts on environmental controls and spatial heterogeneity of soil organic carbon stocks. Biogeosciences 12, 3993–4004. http://dx.doi.org/10.5194/bg-12-3993-2015.
Mueller, K.E., Polissar, P.J., Oleksyn, J., Freeman, K.H., 2012. Differentiating temperate tree species and their organs using lipid biomarkers in leaves, roots and soil. Org. Geochem. 52, 130–141. http://dx.doi.org/10.1016/j.orggeochem.2012.08.014.
Mueller, C.W., Rethemeyer, J., Kao-Kniffin, J., Löppmann, S., Hinkel, K.M., Bockheim, J.G., 2015. Large amounts of labile organic carbon in permafrost soils of northern Alaska. Glob. Chang. Biol. 21, 2804–2817. http://dx.doi.org/10.1111/gcb.12876.
Mueller, C.W., Hoeschen, C., Steffens, M., Buddenbaum, H., Hinkel, K., Bockheim, J.G., Kao-Kniffin, J., 2017. Microscale soil structures foster organic matter stabilization in permafrost soils. Geoderma 293, 44–53. http://dx.doi.org/10.1016/j.geoderma.2017.01.028.
Murayama, S., 1984. Decomposition kinetics of straw saccharides and synthesis of microbial saccharides under field conditions. J. Soil Sci. 35, 231–242. http://dx.doi.org/10.1111/j.1365-2389.1984.tb00279.x.
Muukkonen, P., Häkkinen, M., Mäkipää, R., 2009. Spatial variation in soil carbon in the organic layer of managed boreal forest soil-implications for sampling design. Environ. Monit. Assess. 158, 67–76. http://dx.doi.org/10.1007/s10661-008-0565-2.
Naafs, D.F.W., Nierop, K.G.J., van Bergen, P.F., de Leeuw, J.W., 2005. Changes in the molecular composition of ester-bound aliphatics with depth in an acid andic forest soil. Geoderma 127, 130–136. http://dx.doi.org/10.1016/j.geoderma.2004.11.022.
Neff, J.C., Hooper, D.U., 2002. Vegetation and climate controls on potential CO2, DOC and DON production in northern latitude soils. Glob. Chang. Biol. 8, 872–884. http://dx.doi.org/10.1046/j.1365-2486.2002.00517.x.
Nierop, K.G.J., 2001. Temporal and vertical organic matter differentiation along a vegetation succession as revealed by pyrolysis and thermally assisted hydrolysis and

methylation. J. Anal. Appl. Pyrolysis 61, 111–132. http://dx.doi.org/10.1016/S0165-2370(01)00132-2.
Nordin, A., Schmidt, I.K., Shaver, G.R., 2004. Nitrogen uptake by arctic soil microbes and plants in relation to soil nitrogen supply. Ecology 85, 955–962. http://dx.doi.org/10.1890/03-0084.
Oades, J.M., 1984. Soil organic matter and structural stability: mechanisms and implications for management. Plant Soil 76, 319–337. http://dx.doi.org/10.1007/BF02205590.
Oades, J.M., Osmond, G., Fungalhyphae, E., Iron, G., Periodate, M., Rhizosphere, P., Slaking, R., 1984. Soil Organic Matter and Structural Stability: Mechanisms and Implications for Management Microaggregates Swelling and Dispersion. 337. pp. 319–337.
Otto, A., Simpson, M.J., 2007. Analysis of soil organic matter biomarkers by sequential chemical degradation and gas chromatography – mass spectrometry. J. Sep. Sci. 30, 272–282. http://dx.doi.org/10.1002/jssc.200600243.
Pastick, N.J., Jorgenson, M.T., Wylie, B.K., Rose, J.R., Rigge, M., Walvoord, M.A., 2014. Spatial variability and landscape controls of near-surface permafrost within the Alaskan Yukon River Basin. J. Geophys. Res. Biogeosci. 119, 1244–1265. http://dx.doi.org/10.1002/2013JG002594.
Paterson, E., Gebbing, T., Abel, C., Sim, A., Telfer, G., 2007. Rhizodeposition shapes rhizosphere microbial community structure in organic soil. New Phytol. 173, 600–610. http://dx.doi.org/10.1111/j.1469-8137.2006.01931.x.
Paz-González, A., Vieira, S.R., Taboada Castro, M.T., 2000. The effect of cultivation on the spatial variability of selected properties of an umbric horizon. Geoderma 97, 273–292. http://dx.doi.org/10.1016/S0016-7061(00)00066-5.
Penne, C., Ahrends, B., Deurer, M., Böttcher, J., 2010. The impact of the canopy structure on the spatial variability in forest floor carbon stocks. Geoderma 158, 282–297. http://dx.doi.org/10.1016/j.geoderma.2010.05.007.
Ping, C.L., 2013. Gelisols: part I. Cryogenesis and state factors of formation. Soil Horizons 54, 1–5. http://dx.doi.org/10.2136/sh2013-54-3-gc.
Ping, C.L., Jastrow, J.D., Jorgenson, M.T., Michaelson, G.J., Shur, Y.L., 2015. Permafrost soils and carbon cycling. Soil 1, 147–171. http://dx.doi.org/10.5194/soil-1-147-2015.
Popper, Z.A., Fry, S.C., 2003. Primary cell wall composition of bryophytes and charophytes. Ann. Bot. 91, 1–12. http://dx.doi.org/10.1093/aob/mcg013.
Prietzel, J., Dechamps, N., Spielvogel, S., 2013. Analysis of non-cellulosic polysaccharides helps to reveal the history of thick organic surface layers on calcareous Alpine soils. Plant Soil 365, 93–114. http://dx.doi.org/10.1007/s11104-012-1340-2.
R Core team, 2015. R Core Team. R A Lang. Environ. Stat. Comput. R Found. Stat. Comput., Vienna, Austria. ISBN 3-900051-07-0, URL. http://www.R-project.org/.
Rasse, D.P., Rumpel, C., Dignac, M.F., 2005. Is soil carbon mostly root carbon? Mechanisms for a specific stabilisation. Plant Soil 269, 341–356. http://dx.doi.org/10.1007/s11104-004-0907-y.
Riederer, M., Matzke, K., Ziegler, F., Kögel-Knabner, I., 1993. Occurrence, distribution and fate of the lipid plant biopolymers cutin and suberin in temperate forest soils. Org. Geochem. 20, 1063–1076. http://dx.doi.org/10.1016/0146-6380(93)90114-Q.
Riha, S.J., James, B.R., Senesac, G.P., Pallant, E., 1986. Spatial variability of soil Ph and organic matter in forest plantations. Soil Sci. Soc. Am. J. 50, 1347–1352.
Rodionov, A., Flessa, H., Grabe, M., Kazansky, O.A., Shibistova, O., Guggenberger, G., 2007. Organic carbon and total nitrogen variability in permafrost-affected soils in a forest tundra ecotone. Eur. J. Soil Sci. 58, 1260–1272. http://dx.doi.org/10.1111/j.1365-2389.2007.00919.x.
Rothe, A., Kreutzer, K., Küchenhoff, H., 2002. Influence of tree species composition on soil and soil solution properties in two mixed spruce-beech stands with contrasting history in Southern Germany. Plant Soil 240, 47–56. http://dx.doi.org/10.1023/A:1015822620431.
Ruark, G.A., Zarnoch, S.J., 1992. Soil carbon, nitrogen, and fine root biomass sampling in a pine stand. Soil Sci. Soc. Am. J. 56, 1945–1950. http://dx.doi.org/10.2136/sssaj1992.03615995005600060049x.
Salmon, V.G., Soucy, P., Mauritz, M., Celis, G., Natali, S.M., Mack, M.C., Schuur, E.A.G., 2016. Nitrogen availability increases in a tundra ecosystem during five years of experimental permafrost thaw. Glob. Chang. Biol. 22, 1927–1941. http://dx.doi.org/10.1111/gcb.13204.
Schmidt, M.W.I., Torn, M.S., Abiven, S., Dittmar, T., Guggenberger, G., Janssens, I.A., Kleber, M., Kögel-Knabner, I., Lehmann, J., Manning, D.A.C., Nannipieri, P., Rasse, D.P., Weiner, S., Trumbore, S.E., 2011. Persistence of soil organic matter as an ecosystem property. Nature 478, 49–56. http://dx.doi.org/10.1038/nature10386.
Schöning, I., Totsche, K.U., Kögel-Knabner, I., 2006. Small scale spatial variability of organic carbon stocks in litter and solum of a forested Luvisol. Geoderma 136, 631–642. http://dx.doi.org/10.1016/j.geoderma.2006.04.023.
Schuur, E.A.G., Vogel, J.G., Crummer, K.G., Lee, H., Sickman, J.O., Osterkamp, T.E., 2009. The effect of permafrost thaw on old carbon release and net carbon exchange from tundra. Nature 459, 556–559. http://dx.doi.org/10.1038/nature08031.
Schuur, E.A.G., McGuire, A.D., Grosse, G., Harden, J.W., Hayes, D.J., Hugelius, G., Koven, C.D., Kuhry, P., 2015. Climate change and the permafrost carbon feedback. Nature 520, 171–179. http://dx.doi.org/10.1038/nature14338.
Siewert, M.B., 2015. High Resolution Mapping of Soil Organic Carbon Storage and Soil Properties in Siberian Periglacial Terrain.
Spielvogel, S., Prietzel, J., Auerswald, K., Kögel-Knabner, I., 2009. Site-specific spatial patterns of soil organic carbon stocks in different landscape units of a high-elevation forest including a site with forest dieback. Geoderma 152, 218–230. http://dx.doi.org/10.1016/j.geoderma.2009.03.009.
Spielvogel, S., Prietzel, J., Leide, J., Riedel, M., Zemke, J., Kögel-Knabner, I., 2014. Distribution of cutin and suberin biomarkers under forest trees with different root systems. Plant Soil 381, 95–110. http://dx.doi.org/10.1007/s11104-014-2103-z.
Spielvogel, S., Prietzel, J., Kögel-Knabner, I., 2016. Stand scale variability of topsoil organic matter composition in a high-elevation Norway spruce forest ecosystem. Geoderma 267, 112–122. http://dx.doi.org/10.1016/j.geoderma.2015.12.001.
Stork, R., Dilly, O., 1998. Scale-dependent spatial variability of microbiological characteristics in soil of a beech forest. J. Plant Nutr. Soil Sci. 161.
Streletskiy, D.A., Tananaev, N.I., Opel, T., Shiklomanov, N.I., Nyland, K.E., Streletskaya, I.D., Tokarev, I., Shiklomanov, A.I., 2015. Permafrost hydrology in changing climatic conditions: seasonal variability of stable isotope composition in rivers in discontinuous permafrost. Environ. Res. Lett. 10, 95003. http://dx.doi.org/10.1088/1748-9326/10/9/095003.
Striegl, R.G., Aiken, G.R., Dornblaser, M.M., Raymond, P.A., Wickland, K.P., 2005. A decrease in discharge-normalized DOC export by the Yukon River during summer through autumn. Geophys. Res. Lett. 32, 1–4. http://dx.doi.org/10.1029/2005GL024413.
Tarnocai, C., Canadell, J.G., Schuur, E.A.G., Kuhry, P., Mazhitova, G., Zimov, S., 2009. Soil organic carbon pools in the northern circumpolar permafrost retion. Glob. Biogeochem. Cycles 23. http://dx.doi.org/10.1029/2008GB003327.
Träger, S., Milbau, A., Wilson, S.D., 2017. Potential Contributions of Root Decomposition to the Nitrogen Cycle in Arctic Forest and Tundra. pp. 11021–11032. http://dx.doi.org/10.1002/ece3.3522.
Treat, C.C., Wollheim, W.M., Varner, R.K., Bowden, W.B., 2016. Longer thaw seasons increase nitrogen availability for leaching during fall in tundra soils. Environ. Res. Lett. 11, 64013. http://dx.doi.org/10.1088/1748-9326/11/6/064013.
Van Bellen, S., Dallaire, P.L., Garneau, M., Bergeron, Y., 2011. Quantifying spatial and temporal Holocene carbon accumulation in ombrotrophic peatlands of the Eastmain region, Quebec, Canada. Glob. Biogeochem. Cycles 25. http://dx.doi.org/10.1029/2010GB003877.
Vanguelova, E.I., Bonifacio, E., De Vos, B., Hoosbeek, M.R., Berger, T.W., Vesterdal, L., Armolaitis, K., Celi, L., Dinca, L., Kjønaas, O.J., Pavlenda, P., Pumpanen, J., Püttsepp, Reidy, B., Simončič, P., Tobin, B., Zhiyanski, M., 2016. Sources of errors and uncertainties in the assessment of forest soil carbon stocks at different scales—review and recommendations. Environ. Monit. Assess. 188. http://dx.doi.org/10.1007/s10661-016-5608-5.
Wainwright, H.M., Dafflon, B., Smith, L.J., Hahn, M.S., Curtis, J.B., Wu, Y., Ulrich, C., Peterson, J.E., Torn, M.S., Hubbard, S.S., 2015. Identifying multiscale zonation and assessing the relative importance of polygon geomorphology on carbon fluxes in an Arctic tundra ecosystem. J. Geophys. Res. Biogeosci. 120, 788–808. http://dx.doi.org/10.1002/2014JG002799.
Wang, Y., Hsieh, Y.P., 2002. Uncertainties and novel prospects in the study of the soil carbon dynamics. Chemosphere 49, 791–804. http://dx.doi.org/10.1016/S0045-6535(02)00381-8.
Webb, E.E., Schuur, E.A.G., Natali, S.M., Oken, K.L., Bracho, R., Krapek, J.P., Risk, D., Nickerson, N.R., 2016. Increased wintertime CO2 loss as a result of sustained tundra warming. J. Geophys. Res. Biogeosci. 249–265. http://dx.doi.org/10.1002/2014JG002795. Received.
Weber, P., Bardgett, R.D., 2011. Influence of single trees on spatial and temporal patterns of belowground properties in native pine forest. Soil Biol. Biochem. 43, 1372–1378. http://dx.doi.org/10.1016/j.soilbio.2011.03.015.
Wild, B., Gentsch, N., Čapek, P., Diáková, K., Alves, R.J.E., Bárta, J., Gittel, A., Hugelius, G., Knoltsch, A., Kuhry, P., Lashchinskiy, N., Mikutta, R., Palmtag, J., Schleper, C., Schnecker, J., Shibistova, O., Takriti, M., Torsvik, V.L., Urich, T., Watzka, M., Šantrůčková, H., Guggenberger, G., Richter, A., 2016. Plant-derived compounds stimulate the decomposition of organic matter in arctic permafrost soils. Sci. Rep. 6, 25607. http://dx.doi.org/10.1038/srep25607.
Yang, Z., Yang, S., Van Nostrand, J.D., Zhou, J., Fang, W., 2017. Microbial Community and Functional Gene Changes in Arctic Tundra Soils in a Microcosm Warming Experiment. 8. pp. 1–11. http://dx.doi.org/10.3389/fmicb.2017.01741.
Yuan, M.M., Van Nostrand, J.D., Zhang, J., Xue, K., Wu, L., Deng, Y., Zhou, X., He, Z., Yang, Y., Deng, J., Hale, L., Cole, J.R., Penton, C.R., Tiedje, J.M., 2018. Microbial Functional Diversity Covaries with Permafrost Thaw-induced Environmental Heterogeneity in Tundra Soil. pp. 297–307. http://dx.doi.org/10.1111/gcb.13820.
Zar, J.H., 1984. 3.6 Serial randomness of nominal scale categories. In: Biostatistical Analysis, pp. 418–419.
Zollinger, B., Alewell, C., Kneisel, C., Brandová, D., Petrillo, M., Plötze, M., Christl, M., Egli, M., 2017. Soil Formation and Weathering in a Permafrost Environment of the Swiss Alps: A Multi-parameter and Non-steady-state Approach. 835. pp. 814–835. http://dx.doi.org/10.1002/esp.4040.
Zubrzycki, S., Kutzbach, L., Grosse, G., Desyatkin, A., 2013. Organic carbon and total nitrogen stocks in soils of the Lena River Delta. Biogeosciences 10, 3507–3524. http://dx.doi.org/10.5194/bg-10-3507-2013.